jntes

JOURNAL OF NEW TECHNOLOGIES IN ENVIRONMENTAL SCIENCE

3

2020

No. 3 Vol. 4 ISSN 2544-7017 www.jntes.tu.kielce.pl Kielce University of Technology

CONTENTS

www.jntes.tu.kielce.pl
jntes@tu.kielce.pl

The quarterly printed issues of Journal of New Technologies in Environmental Science are their original versions. The Journal published by the Kielce University of Technology.

ISSN 2544-7017

Doi: 10.53412

Larissa TRETIAKOVA
Ludmila MITIUK
National Technical University of Ukraine "Igor Sikorsky Kyiv Polytechnic Institute", Ukraine

DOI: 10.53412/jntes-2020-3.1

ENVIRONMENTAL SAFETY EVALUATION FROM GALVANIC SLUDGE DURING LONG-TERM STORAGE

Abstract: *The article analyses the ecological state of the soil in an enterprise with a galvanic shop that produces chips and microcircuits. The problem of production waste storage in open areas is investigated. Environmental hazards during long-term storage of sludge have been identified. The composition of the sludge obtained after sewage treatment of the production of the copper line was investigated. A method for predicting the level and depth of soil salinity during long-term sludge storage is proposed. The experience of reuse of copper extracted from sludge is analysed.*

Keywords: *galvanic production, sludge, soil salinity, prediction.*

Introduction

Implementation of environmental security is accepted as a basic component of national security for Ukraine, taking into account the systematic nature of environmental problems and their correlation with economic, political and social factors. Under the influence of many anthropogenic factors, a certain ecological environment is formed. Numerous scientific studies [6] indicate that genetically programmed mechanisms of regulation of human behaviour are not adapted quickly enough to the conditions of increasing influence of anthropogenic loads. Extra loads on the human body due to poor food, contaminated water and the atmosphere lead to the nervous and endocrine systems damage. Such factors create favourable conditions for the development of traditional diseases and cause new types of serious ailments in humans and animals: atypical pneumonia, influenza, hepatitis, Ebola and others. Anthropogenic pressure on the environment acts as an independent stress factor, which results in various conflicts in society. Neglecting environmental safety in Ukraine for many years has led to uncontrolled consequences:

- economic: reduction of total production volumes, deterioration of living standard; increase in the number of industrial accidents;
- political: increasing distrust of state structures; inability to effectively counter external economic and military aggression;
- medical: increasing the level and complexity of occupational diseases, which results in loss of working capacity in the able-bodied population; stress; nervousness in relationships, demographic situation worsening.

One of the first places among environmental problems is the problem of water resources [4]. In Ukraine, surface water is polluted mainly by petroleum products, phenols and heavy metals. The most polluted waters are recorded in the Dnieper basin, in the rivers Ros, Goryn, Sluch, Teteriv and others, on the banks of which large industrial enterprises and cities are located [11]. The content of pollutants in these rivers is accordingly: petroleum products – (10, …, 18) maximum permissible concentrations (MPC); phenol – (1, …, 5) MPC, copper compounds – (4, …, 17) MPC, zinc – (20, …, 28) MPC.

Groundwater is subjected to significant techno-genic effects. In the valleys of Siverskyi Donets, the rivers of the Western Donbas, the Kryvyi Rih basin, the Carpathian region, more than 200 centers of permanent pollution of water soil horizons have been fixed. To date, this irresponsible attitude towards the disposal of industrial waste has resulted in complete contamination of 6% and partial contamination of 25% of explored groundwater reserves. Today, in conditions of military aggression in the territories of the Donbas that are temporarily occupied, the pollution levels of the Siverskyi Donets, Krynka and groundwater rivers are at a catastrophic level due to the discharge of untreated liquid industrial waste [16].

Water pollution is inseparably linked to soil pollution. Substantial environmental damage is caused by soils due to their pollution by liquid and solid industrial production. Solid waste, consisting of waste from metallurgical, chemical, electroplating industries, and from mining and mineral processing, is often located on agricultural land. Such wastes are a source of toxic substances and elements that enter the atmosphere, soil, surface and groundwater, causing irreparable damage. In Ukraine, an average of 1 680 million tonnes of solid waste of industrial enterprises are accumulated annually which must be processed, disposed of and stored.

According to the Law of Ukraine "On Environmental Protection" [9], an environment is considered to be safe if its condition meets the statutory criteria, standards and allowances. In accordance with the sanitary norms, requirements have been approved that determine its qualitative and quantitative levels of contamination and resource content.

The scale of the annual production and accumulation of solid waste requires the creation of powerful processing plants, which productivity is measured in millions of tons per year. The problem of practical implementation of scientific and technical developments is associated with numerous difficulties of financial, social and technical nature. The problem of industrial waste recycling is an urgent one, caused by the constant increase in the amount of waste and insufficient rates of its processing.

Waste containing heavy metals is of particular danger. Such contamination of the soil and water occurs near the enterprises with galvanizing plant. Galvanic production is used previously to various coatings: chromium plated, copper, nickel plated, galvanized. Such productions in Ukraine are located at the enterprises of the military-industrial complex, machine building and electronic equipment.

Galvanic production consists of sequential electrochemical processes (galvanizing, nickel plating, chromium, copper plating). As a production result, waste is generated: electrolytes and etching solutions of different composition. Mixed with water during the purification, the electrolytes and etching solutions form toxic wastewater. Heavy metals trapped in water and absorbed by phytoplankton are of particular danger, which can subsequently lead to their ingestion. Regulatory documents set maximum permissible concentrations for metals that get into water [8].

Dry waste (sludge) is formed during wastewater treatment. The most dangerous components of sludge are heavy metal oxides. Depending on the technological features in the waste of various galvanic industries, heavy metals were fixed within the following limits: copper – (500, …, 5600) mg/kg, iron – (750, …, 1100) mg/kg, chromium (250, …, 5000) mg/kg, nickel – (20, …, 200) mg/kg, zinc – (100, …, 5500) mg/kg, lead – (130, …, 600) mg/kg, tin – (1200, …, 7600) mg/kg [2]. Due to the variety of chemical elements in the sludge and the high level of harmfulness, the problem of their storage, disposal and recycling arose. The difficulty in galvanic waste recycling is that the waste contains different metals, depending on which different technologies are used. For example, the use of the method of electrical coagulation during the treatment of galvanic line sewage. Ferrite method of sewage treatment of galvanic production is based on the reaction of iron oxides formation, in the process of which there is a simultaneous deposition and sorption of heavy metal ions. Improving the precipitation structure makes it possible to intensify the process of separating it from water [10].

However, the issue of storage, purification and reuse of sludge in the production area receives current attention. The reasons for this condition are the lack of a methodology for assessing the contamination levels and effective methods of metal recovery and recycling. Nowadays, the most common ways of using sludge is to add it as a raw material for the production of expanded clay, brick and ceramic tile

and to obtain coloured glaze, which is further used in ceramic products. However, a small amount of sludge is recyclable. This results in an annual formation of up to 12000 tonnes of sludge in the territories of Ukrainian enterprises [7].

Long-term storage of galvanic waste is allowed at special sites in equipped storage facilities. However, as practice shows, artificial repositories have limited capacity and service life. Nowadays, the sludge is stored in open areas with the use of protective coating materials made of clay, polyethylene, polyvinyl chloride. The large waterlogging of territories and the loose permeable soils in Ukraine complicate the choice of landfills for industrial waste and limit their area. Solid wastes under the influence of precipitation, especially acid rain, go into a liquid state. Such phenomena lead to the leakage of reactive elements into the environment. As a result, heavy metal contamination occurs not only adjacent to the soil and surface water storage sites, but also to groundwater horizons. The levels of soil and water pollution in the regions of Ukraine where galvanic and painting shops are located are significant [15].

Contamination of the soil surface brings a number of problems related to soil salinization, soil water contamination and increased water mineralization in surface water bodies. According to the degree of salinization, the soils are divided into weak, medium, strong, and extremely strong saline [5]. It is established that on poorly saline soils the crop yield decreases on average to 25%, on medium-saline soils – up to 50%, on strongly saline soils – up to 75%. Soils with a level of salinity in excess of 75% become practically unsuitable for plants of all kinds and sorts. Regardless of the chemical composition of substances, salts can concentrate in a certain soil horizon. According to the depth of the salt layer from the surface, the soils are divided into four types: surface salinization (0, …, 30) cm; medium salinization (30, …, 80) cm, deep salinization (80, …, 150) cm and depth (very deep) salinization (>150) cm soils. In 2017 there were 4700 million m^2 of medium and heavily saline soils in Ukraine, accounting for 14.3% of agricultural land [1].

Predicting the development of hazardous physical and chemical processes on the surface and deep soil layers is one of the basic requirements for environmental safety. Solving the problem of limiting the negative impact of industrial waste makes it possible to significantly improve working and living conditions for people.

It is important to develop a method for predicting soil salinity levels and the possibility of groundwater contamination by galvanic waste.

Purpose and research objectives

The article is devoted to the analysis of the ecological status of the territory of the enterprise with the electroplating workshop, which produces chips and microcircuits. The purpose of the article is to improve the method of predicting the effect of galvanic sludge on soil salinity and groundwater contamination.

To achieve this goal, one needs to solve the following problems:

1. To analyse the experimental data on the qualitative and quantitative composition of the sludge that are formed in the galvanic shop during the chips production.
2. To develop a mathematical model of the distribution process of heavy metals, high-density metals in the soil, which lead to salinity of the soil and pollution of groundwater. Based on the model, create a methodology for predicting the depth and concentration of contamination.
3. Check the reliability of the developed mathematical model and methodology, created on its basis.
4. Suggest proposals for implementation of the obtained results.

Research matter and results

Copper is widely used in chips and microcircuits production and electroplating because of its high electrical conductivity. The article investigates the production processes of “copper etching” during chips and microcircuits manufacturing. The process of “etching copper” is used to create and secure

the images on the surfaces of chips and microcircuits. The processing of individual parts is accompanied by the use of a large amount of water and, accordingly, the generation of waste. The spent technological solutions of chemical and electrochemical degreasing, as well as alkaline sewage, after cascading washing, fall into acidic drains. The spent electrolyte of the copper line is partially directed to regeneration and the recovered solution is reused in the technological process.

The technological processes in the galvanic shops promote the formation of liquid waste with metals in the process of digestion and solid waste (sludge) – during disposal.

Experimental data

The authors carried out experimental studies of the sludge accumulation process at the enterprise during the operation of copper etching lines during chips and microcircuits manufacturing. The research was carried out on the territory of the enterprise for the production of electronic equipment in Cherkasy region of Ukraine. The company has been operating for 48 years. The average production capacity is up to 2500 m^2 of chips per month. With the productivity of the digestive line 14 m^2/h, the amount of sludge in 8 hours reaches (100, ..., 120) kg. For one month during work in one shift accumulates up to 2500 kg and for two shift work – up to 5000 kg. According to the analysis of chip production waste, the percentage of a number of metals was determined (Table 1).

TABLE 1. *Metal content of the sludge in test specimens*

Indicators	**Metal content in sludge**					
Type of metal bond	CuO copper	CaO calcium	Fe_2O_3 iron	Cr_2O_3 chromium	NiO nickel	ZnO zinc
Metal content, %	16	8	9	2	2	1
Harm class	3	4	3	3	3	3
Limit concentration in water, mg/dm^3	1.0	3.5	0.3[3]	0.05	0.1[3]	1.0

The enterprise, which productivity ranges from 2.000 m^2 to 4.000 m^2 of chips, accumulates from 30 tonnes to 48 tonnes of waste annually. In previous years, the sludge was stored on the territory of the enterprise in landfills in open areas. For the last 20 years, the sludge has been stored in polyvinylchloride packages.

Storing sludge with particle sizes (0.1, ..., 50) μm with metal oxides, the soil is salted and this has the corresponding negative effects. Under the influence of atmospheric precipitation, metal ions are washed out and transferred to soils, surface and ground waters due to easy dissolution in acidic environment. The zone of aeration of the soil is saturated with salts of metals, which gradually move to the groundwater level. Soil salinity is measured as a percentage of the dry soil density: in the presence of metal salts, less than 0.1% of the soil is considered unsalted; (0.1, ..., 0.3)% – poorly salted; (0.3, ..., 0.5)% – average salinity; (0.5, ..., 0.75)% – strongly salted.

Model description

A method for predicting soil contamination in the sludge storage area is proposed. Simulation of the process of movement of salts from the surface of the earth to the below-located layers of the zone of aeration occurs according to the laws of molecular diffusion.

Soils in the area have the following structure: loam – $h_1 \leq 1.5$ m; sand – $h_2 \leq 0.3$ m; groundwater – $h_3 \leq 0.8$ m; clay – $h_4 \leq 1.2$ m; then the interlayer water begins (Fig. 1). The pores are up to 40 per cent of the volume of the soil layer.

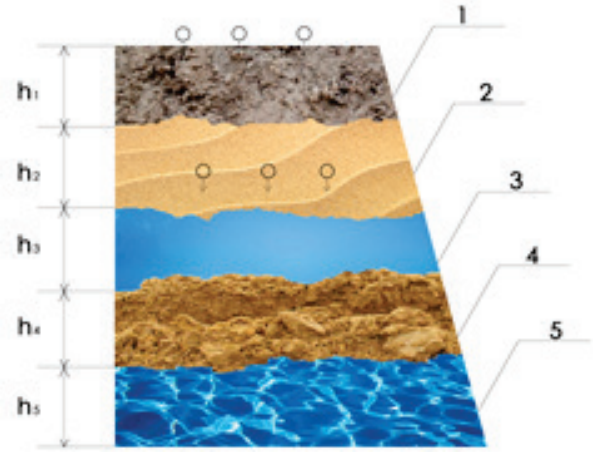

Figure 1. *Structural diagram of the soil: 1 – loam, 2 – sand, 3 – groundwater, 4 – clay, 5 – interlayer water*

The research methodology is based on the use of the theory of physicochemical hydrodynamics of porous media. The process of metal salts cycling can be described by the differential equation of motion and the conservation of mass of matter for the vertical transfer of mass of matter [12]. The presence of sludge on the soil surface corresponds to the first-order boundary condition.

$$D\frac{d^2C}{dX^2}=\theta\frac{dC}{dT} \tag{1}$$

where:

D – molecular diffusion coefficient, m²/s;

C – salinity of rocks, %;

θ – volume humidity, %;

X – the spatial coordinate, m;

T – time coordinate, s.

The analytical solution of equation (1) has the form:

$$C_{hx}=\left(C_s-C_0\right)erfc\frac{1}{2}\frac{h_x}{\frac{D\cdot T}{\theta}} \tag{2}$$

where:

C_{hx} – the predicted level of salinity at a depth of h_x, %;

C_s – surface salinity of the aeration zone at h = 0;

C_0 – initial level of soil salinity before the start of storage at T = 0;

h_x – distance of the calculated points from the origin, i.e. from the surface of the earth, m;

T – term of the predicted calculation, year;

$erfc$ – tabulated function.

The predicted salinity level is determined by the following target setting:

1. The level of salinity for 20 years during the sludge storage in the open area.
2. Salinity level for 20 years during the packed sludge storage in an open area.

In the course of prediction, the following assumptions are made: the process of accumulation of metals is cumulative; annual seasons of soil moisture change are not taken into account. One year (365 days) is accepted for the billing period. The total prediction time is 20 years.

Input data

The molecular diffusion coefficient D characterizes the movement of metal ions as a result of thermal motion in the soil and depends on the properties of the metal molecules, temperature and pressure. In the calculations, the reference value D was taken at a temperature of 20°C [14].

Volume humidity θ is determined by the moisture content of the soil and is calculated by the formula:

$$\theta = \frac{m_{sw}}{\left(V_{hs} + V_{is} + V_{sw}\right)} \tag{3}$$

where:

m_{sw} – mass of water in the soil;

V_{hs} – volume of hard soil;

V_{is} – volume (interstices of soil) of pores;

V_{sw} – volume of subsoil water.

At the first formulation of the problem, the following baselines were adopted:

- salinity of the soil surface prior to the beginning of storage is C_0 = 1%;
- the soil has pores up to 40% of the volume. We accept the maximum value of C_s = 40% on the boundary of "air – soil surface", which corresponds to a constant layer of slag on the soil surface;
- the molecular diffusion coefficient is defined as the mean value per day $D = 1 \cdot 10^{-5}$ m²/day;
- volumetric humidity is taken as the average value during the year θ = 0.23.

In the second formulation of the problem, it is necessary to consider changes in the levels of surface salinity during the calculation period, i.e. $C_s\big|_{h=0} \rightarrow$ var.

Sludge storage in polyvinyl chloride packages results in gradual contamination of the surface layer. This is due to packaging damage, primarily due to the failure of the joints obtained by high-frequency welding. Seams under the influence of mechanical stress, changes in external temperatures, UV radiation and precipitation are cracked, which leads to the formation of a constant layer of sludge in the storage areas. It should also be noted that the guaranteed service life of this type of packaging does not exceed 15 years.

The value of the surface salinity of the soil is determined based on the results obtained in the previous iteration:

$$C_s\big|_{h=0}^{i} = C_0\big|_{T=0} + \Delta C_s\big|_{h=0}^{(i-1)} \tag{4}$$

where:

$C_s\big|_{h=0}^{i}$ – level of soil salinity on the surface in the i-th iteration;

$C_0\big|_{T=0}$ – tinitial level of soil salinity before the start of storage at T = 0;

$\Delta C_s\big|_{h=0}^{(i-1)}$ – increase in the level of salinity of the soil surface during storage of sludge during the previous year, which corresponds to (i–1) iteration.

Predicting the salinity depth, the calculation points are selected in 0.1 m steps from the surface.

Results

The first formulation of the problem calculates the annual changes in soil salinity levels by the depth of penetration. The results of changing the depth of penetration of metals into soil layers by years are shown in Figure 2.

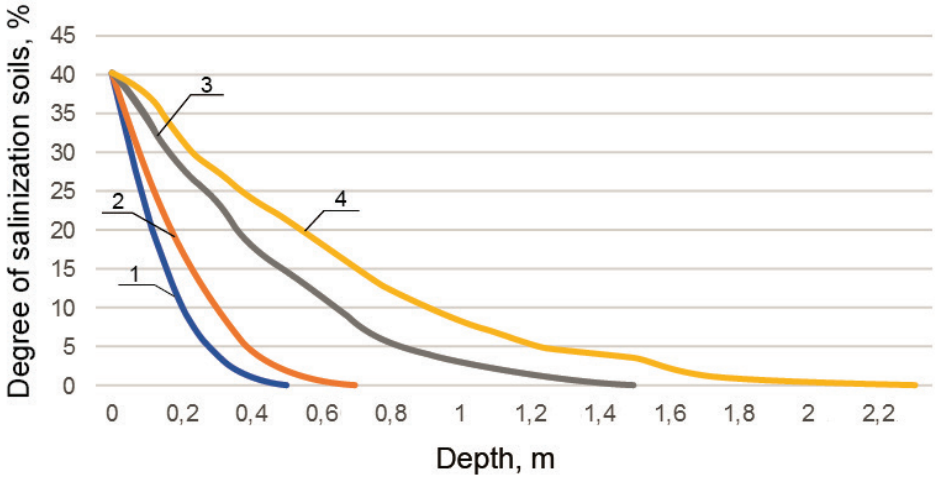

FIGURE 2. *The level of soil salinity at the depth of penetration during storage of sludge in the open area: 1 – one year storage, 2 – five years, 3 – ten years, 4 – twenty years*

According to the graphs (Fig. 2), the storage of sludge in open areas annually results in the increase in the depth of soil salinity.

Storing the sludge in polyvinyl chloride packing, a long-term soil contamination prediction is obtained as a result of an iterative calculation according to formula (2). The level of soil salinity decreases substantially in the first ten years of storage, but complete soil protection is not ensured (Fig. 3).

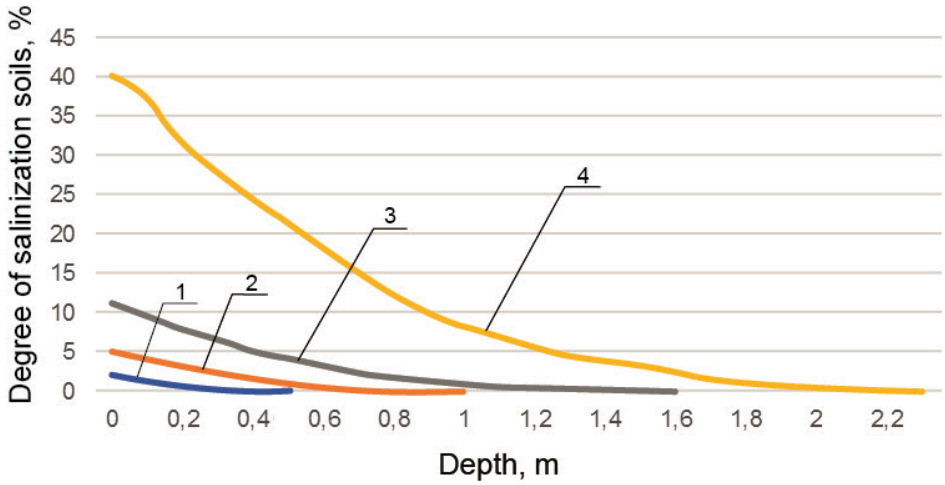

FIGURE 3. *The level of soil salinity at the depth of penetration during storage of sludge in the package: 1 – one year of storage, 2 – five years, 3 – ten years, 4 – twenty years*

As shown in Figure 3, the soil salinization process is slowed down during storage of the sludge in polyvinyl chloride packing, but practically reaches the previous levels due to the destruction of the packing after 20 years.

According to the force regulations, the salinity level exceeding 0.3% is already a danger to the environment. Figure 4 shows the soil depth with a salinity level of (0.3, …, 0.344)% during long-term storage of sludge in open areas.

As follows from Figure 4, when the sludge is placed on the open surface in a year, the soil 0.65 m thick goes into the category of poorly saline, in four years such a layer reaches a depth of 1 meter, in 15 years the depth reaches two meters, which creates conditions for groundwater contamination. The contamination process is slower when the sludge is stored in the package. However, if the service life exceeds 15 years, the process of polymer destruction packaging takes place and further storage leads to contamination of soil and groundwater.

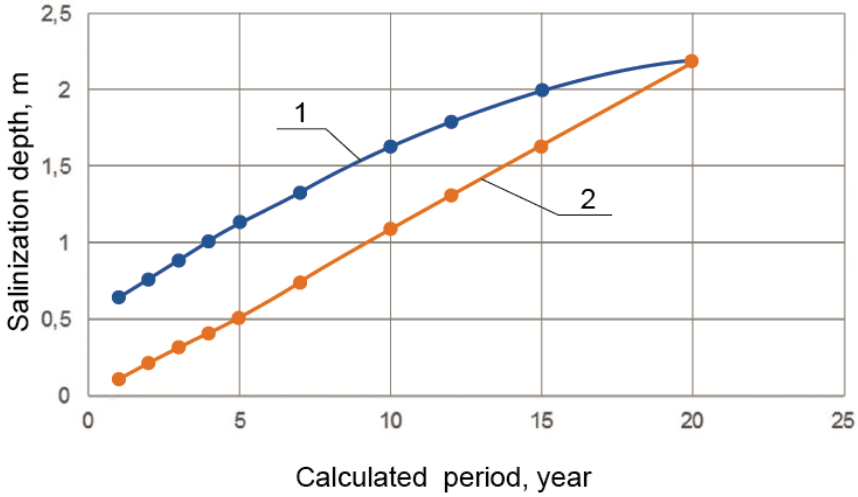

FIGURE 3. *Depth of distribution of soil salinity within C_{hx} = (0.3, ..., 0.344) during long-term storage in the open area: 1 – storage of sludge without packaging, 2 – storage of sludge in polyvinyl chloride packaging*

Future work will be dedicated to developing and implementing effective wastewater treatment and sludge extraction methods. Ukraine has a high demand for copper, which is used in the electrical, aircraft, and defense industries. Prospective deposits of copper ores have been discovered in the Volyn region, on the Donbass in the Dnipro-Donetsk surface valley. The total resources of ores of the Volyn region are estimated at 28 million tons of metal with an average copper content of 1.0%. Ukraine's annual demand for copper is (120, ..., 140) thousand tons, twenty per cent of which is provided with its own copper scrap, and additional ones in the form of raw copper are imported from Poland [3]. In the current economic and technological conditions, it is advisable to use sludge as a secondary raw material. The required copper raw material can be obtained by galvanic wastewater treatment.

Nowadays in Ukraine, up to 20% waste and extraction of mineral resources and sludge are reused. Many countries around the world have accumulated the experience of disposal and sludge metals, including electroplating. For example, in Germany the reuse of iron reaches up to 38%, tin – 34% and zinc – 33%; in the USA copper reaches up to 43%, in the UK – lead 60%, aluminum – 33% [13]. As the results of the research showed, the separated copper from wastewater meets the requirements of industrial production. Copper can be used for smelting or metallization in appropriate processes.

Conclusion

1. On the basis of full-scale research at the enterprise for the manufacture of chips and microcircuits of the process of accumulation of sludge during the operation of the "copper etching" lines the conditions of their storage are analysed. It was found that the sludge samples contained heavy metal oxides: copper up to 16%, iron up to 9%, chromium up to 2%, nickel up to 2%, zinc 1%.
2. A method for predicting the depth of penetration of heavy metals and increasing the level of soil salinization based on the theory of physical and chemical hydrodynamics of porous media is proposed.
3. Information on soil structure and its characteristics (molecular diffusion coefficient, volume humidity), annual volumes and conditions of sludge storage within the enterprise were used as initial data for prediction.
4. According to the results of the calculations it is determined:
   - during the placement and storage of sludge in the open area for a year, the soil 0.65 m thick goes into the category of poorly saline, in four years such a layer reaches a depth of 1 meter, in 15 years the depth reaches two meters, which creates conditions for groundwater contamination;

- during the use of packaging made of polyvinyl chloride to save the sludge, the contamination process is slower. However, if the service life exceeds 15 years, the process of polymer destruction packing takes place and further storage leads to soil and groundwater contamination.

Conflicts of Interest: The author declares no conflict of interest.

REFERENCES

[1] Baliuk S., Nosonenko A., *Classification of the Ukrainian irrigated soils in accordance with a level of their salinization, alkalinization and alkalinity*, Journal of Soil Science, 2008, Vol. 9, 1, pp. 27-31.

[2] Bondarenko I.V., Anischenko L.Y., Rudyk Y.I., *Substantiation for enhancement of environmental safety of waste management systems through forecasting efficiency of specialized equipment*, Visnyk of Lviv State University, 2017, 2 (16), pp. 119-128.

[3] Chervonij I., Bredihin V., Gritsaj V., Ignatyev V., Ivashchenko V., *Non-ferrous metallurgy of Ukraine*, monograph, ZDIA, Zaporizhzhya, 2014, p. 380.

[4] Directive 2000/60/EC of the European Parliament and of the Council of 23 October 2000 establishing a framework for Community action in the field of water policy, 2000, Official Journal of the European Communities, L 327, Vol. 43, pp. 68-72.

[5] DSTU 3866-99, 1999, Soils. Classification of soil by level of secondary salinity, State Standard of Ukraine, Kyiv, p. 6.

[6] Dudyuk V., Gobela V., *Some theoretical approaches to the definition of environmental security*, Visnyk NLTU of Ukraine, 25, 2015, pp. 130-135.

[7] Kanilo P., *Greenhouse effect. Man-made environment*, Visnyk of HN Road-transport University, Kharkiv 2015, p. 312.

[8] Code of Ukraine about depths. Forest Code of Ukraine. Water Code of Ukraine, Paluvoda, Kyiv 2015, p. 180.

[9] Law of Ukraine. About environmental protection. Water conservation, 1994, State Standard of Ukraine, Kyiv, p. 64.

[10] Melnik O., *Galvanic sludge*, Visnyk (journal) of Sumy National University, 2011, 46, pp. 185-189.

[11] National report on the state of the natural environment in Ukraine, Kyiv 2018, Ministry of Environment and Natural Resources, p. 350.

[12] Nigmatulin R., *Multiphase Environment Dynamics*, Nauka, Moskva 1987, p. 360.

[13] Nester A., Rogov V., *Wastewater renovation of circuit board manufacture*, Visnyk of Sankt-Peterburg University, The series of books: Physics and Chemistry, 2015, pp. 72-79.

[14] Polovij A., Gutsal A., Dronova O., *Soil science*, monograph, Ekologiyu, Odessa 2013, p. 668.

[15] Protasenko O.F., Ivashura A.A., *The role of a healthy environment in creating safe conditions for human activity, Information and Communication Technology*, 80, HAI, Kharkiv 2018, pp. 210-216.

[16] Serdyuk S., Lunova O., Ahieva O., Kamianska V., *Small rivers of Ukraine*, Journal of Donetsk Mining Institute, 2017, 1 (40), pp. 101-106.

Sylwia JANTA-LIPIŃSKA
Koszalin University of Technology

DOI: 10.53412/jntes-2020-3.2

EXPERIMENTAL AND THEORETICAL STUDIES OF NOx EMISSION REDUCTION DURING THE COMBUSTION OF GASEOUS FUEL IN THERMAL POWER BOILERS

Abstract: *The nitrogen oxides in a flame of burning fuel can be created by many mechanisms. The amount of NO_x concentration emitted to the ground atmosphere mainly depends on the type of fuel burned in the industrial and heating boilers. Changes in the country's thermal policy and requirements that are set for us by the European Union States are forcing us to reduce greenhouse gas emissions. Directed metered ballast method is one of the most attractive techniques for reducing NO_x emissions. In recent years, moisture injection technology is still investigated on low and medium power thermal power boilers operating on gaseous fuel. The goal of this work was to perform the investigations of the process of a moisture injection into the zones of decisive influence (SDW-I and SDW-II) on steam and water boilers: DKVR 10-13, DKVR 20-13, DE 25-14 and PTVM-50. The obtained results clearly show how the proposed method affects NO_x reduction and boiler efficiency.*

Keywords: *emission, combustion, dosed directional ballasting method, mono flame, nitrogen oxides.*

Introduction

Currently, the Polish heat management works mainly on solid fuel [7, 11, 12]. Such a policy causes more and more technical, economic and ecological problems due to the conditions set for us by the European Union countries [25, 26, 31]. Recently, the Polish government announced the country's heat policy program in the perspective of 2040. It assumes, among others transition of heat management from solid fuel to natural gas. Therefore, the challenge for Polish heating is the effective and environmentally friendly transition (switching) of thermal energy from solid fuel to gaseous fuel. These are devices called "low energy" due to their age are characterized by low efficiency and a significant impact on the level of environmental pollution in the ground layers of the atmosphere [32, 34]. The exhaust gas from these devices is discharged into urban development zones through small chimneys. The EU regulations obliging all European Union countries, including Poland, to reduce greenhouse gas emissions are not without significance here.

The combustion of organic fuel is accompanied by the formation and emission of toxic and carcinogenic substances into the atmosphere. In addition to nitric oxide, exhaust gases may contain carbon monoxide, aldehydes, organic acids and other carcinogenic compounds. The harmful importance of these pollutants for the natural environment is emphasized by the fact that they are legally limited. The emission of nitrogen oxides or dust depends on the type of fuel burned [1, 28, 29]. Each of these substances has a different quantitative composition and poses a different danger to man and the environment. During the combustion processes, the construction details and technological conditions affect the concentration of harmful components contained in the exhaust gas to varying degrees. For example, when burning gaseous fuel containing no sulfur, the emission levels of harmful substances contained in the exhaust gas are as follows [15]:

- benzapyrene 0-20 µg/100 m^3,
- carbon monoxide 70-100 mg/m^3,
- sulphur dioxide 0 mg/m^3,
- nitrogen oxides 100-400 mg/m^3.

The above statement shows that mainly oxide and nitrogen dioxide (NO_x) determine the level of environmental performance of boiler equipment when burning gaseous fuel [6, 19, 20, 22].

Formation mechanisms and methods for the suppression of nitrogen oxides

The concentration of nitrogen oxides in the exhaust gas depends on the maximum temperature of the combustion process, the concentration of oxygen in the combustion zone, the residence time of the reacting mixture in the maximum temperature zone, and on the nitrogen content in the fuel. Depending on the combination of these parameters, NO_x emissions in flue gas may oscillate from 0.1 g/m^3 to 2 g/m^3.

In the literature there are three mechanisms for the formation of nitrogen oxides in a flame of burning fuel distinguished [2, 33]:

- thermal – which is formed as a result of high temperature oxidation of nitrogen from the air;
- prompt – formed in the initial combustion zone by chemical reactions with the participation of CH and CH_2 radicals. There is also a known in the literature hypothesis regarding another possible mechanism for the formation of nitrogen oxides in an organic fuel flame (the so-called "impact"), which otherwise explains the difference between the content of nitrogen oxides and the thermal mechanism of their formation [21];
- fuel – produced with the participation of chemical compounds containing nitrogen and included in the fuel.

Figure 1 shows a diagram of the formation of nitrogen oxides in the range of temperatures characteristic of boiler furnaces. In some cases, the formation of nitrogen oxides occurs predominantly by one of three mechanisms. For example, when burning gas in low-power devices, the so-called "prompt" NO_x prevail, whereas in fluidized coal combustion the "fuel" ones. The combustion of gaseous fuel in the furnaces of boilers is accompanied by the formation of thermal and prompt nitrogen oxides.

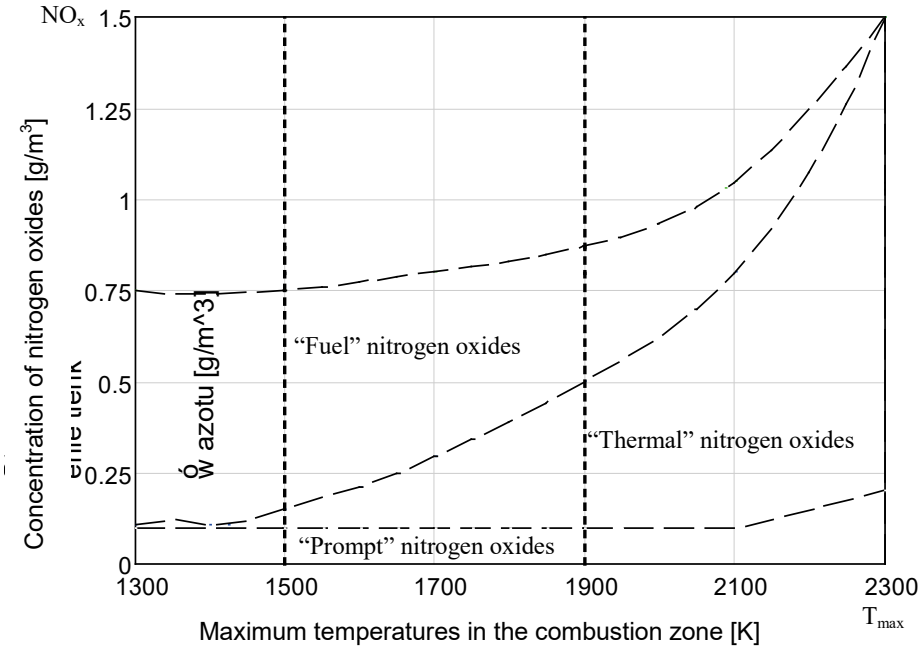

Figure 1. *Dependences of the concentration of nitrogen oxides, as a function of maximum temperatures in the combustion zone, divided into characteristic zones of the influence of NO_x formation mechanisms*

The main directions of research in the field of suppressing nitrogen oxide emissions, taking into account the thermal mechanism of their formation, was the reduction of the maximum temperature and oxygen concentration in the combustion zone.

This can be achieved by:

- combustion with reduced α,
- exhaust gas recirculation,
- moisture injection,
- multistage combustion.

Author in the composition of an international research team headed by prof. Szkarowski has been involved in the use of combustion methods with reduced α and moisture injection for many years. It should be emphasized that these two ways often complement each other. This article summarizes a number of experimental and theoretical studies in these two methods [4, 16, 18-20].

Theoretical research

The method of water ballast injection is considered one of the most promising scientific and technical solutions aimed at reducing atmospheric pollution by harmful products of organic fuel combustion [16, 17, 23, 24]. Compared to other atmosphere protection technologies, the injection method is characterized by unique energy-ecological and technical-economic indicators [5, 13].

As a result of the conducted research, the following two issues were analyzed. The first of these was to determine the detailed structure of the flame in terms of the processes of nitrogen oxides (NO_x) production that occur. This was to ensure optimal ballasting of the zones where the processes take place [3]. The second issue was to explore the possibility of intensifying processes within the flame to maximize the reduction of the excess air supplied for combustion and to reduce the value of heat loss with exhaust gases.

I.J. Sigal divided the combustion process into four temperature zones [15] that determine the formation of nitrogen oxides (Fig. 2). Zone I is the zone where the maximum temperature in the combustion zone reaches up to 750 K. In turn, zone IV is the maximum temperature in the combustion zone reaching the limit above 2500 K. The author of this division recognized that for the processes occurring in the furnaces of boilers, the temperature conditions of the zones occurring in the so-called III a and III b zone are characteristic.

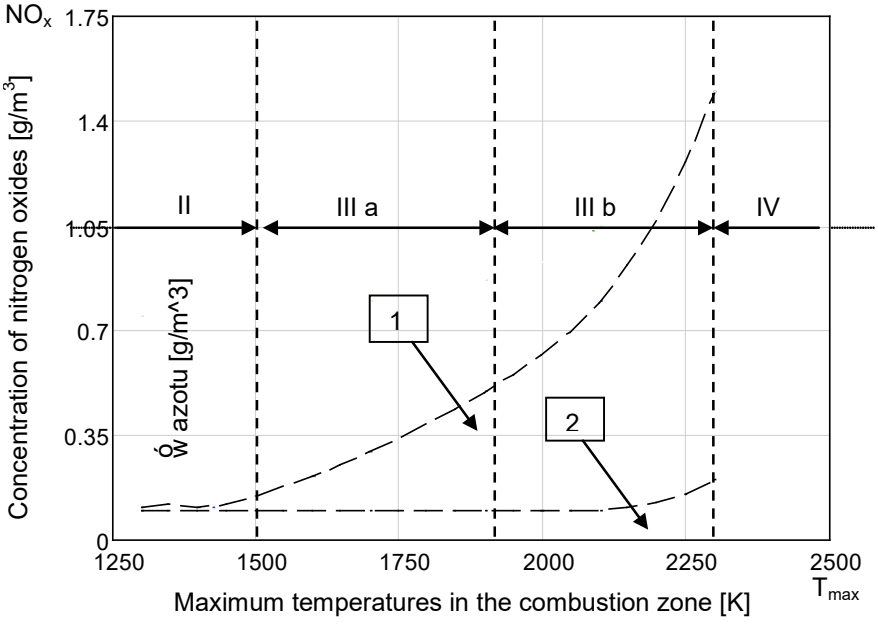

Figure 2. *Dependences of the concentration of nitrogen oxides as a function of maximum temperatures in the combustion zone, divided into zones of influence according to Sigal*

Another division was proposed by L.M. Tsyrulnikow, namely the division of the flame structure into four zones depending on the relative length of the flame [27] (Fig. 3):

- zone A_1 – from the place of flame outlet from the cross section of the burner to the cross section of the furnace where the temperature is 1650 K (it is the temperature at which the concentration of thermal nitrogen oxides reaches the value of 1 mg/m^3);
- zone A_2 – from the above-mentioned section to the place where the maximum temperature in the flame is obtained, where the intensity of nitrogen oxidation from air reaches a maximum;
- zone B – from the cross-section with the maximum temperature in the combustion zone to the cross-section with the "critical" temperature of 1650 K, where combustion of combustible components usually ends, and the concentration of "air" NO_x reaches its maximum value;
- zone C – from the section mentioned above to the exit from the furnace, where there are no significant changes in the concentration of nitrogen oxides.

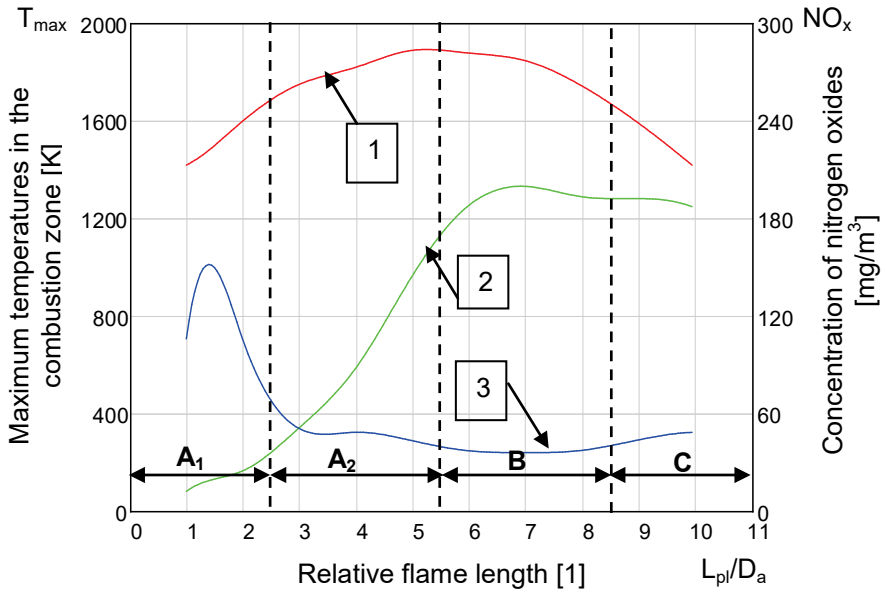

FIGURE 3. *Dependences of the maximum temperature in the combustion zone (1) and concentration of nitrogen oxides (2-thermal, 3-prompt) in flame as a function of relative flame length*

On the other hand A.A. Jemieljanow distinguishes, in the resulting flame, the zones of intensive generation of nitrogen oxides (SIG) [5]. The zones he separates are treated as intervals for achieving local temperature maxima.

The author has attempted to jointly consider and mutually enrich the flame structure analysis proposed by Sigal, Tsyrulnikow and Jemieljonow. This allowed to formulate the concept and separate two zones of decisive influence (SDW), which determine the possibility of active influence on various processes occurring in the flame, also the mechanisms of nitrogen oxide formation:

- SDW-I which includes a significant part of zone A_1, in which by introducing water ballast you can control the processes taking place in this flame zone in order to affect the conditions determining the intensity of further NO_x production by non-thermal mechanisms of its formation (i.e. prompt, impact);
- SDW-II is the zone of maximum temperatures at the junction of zones A_2 and B, in which both ballasting and controlling the excess air coefficient enables throttling of the thermal mechanism of nitrogen oxidation. An overview diagram of the flame as a result of such analysis is shown in Figure 4.

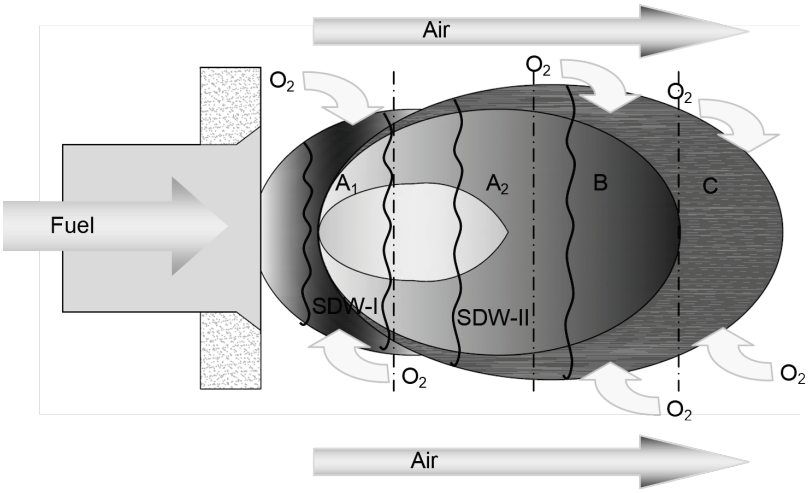

FIGURE 4. *Schematic diagram of the structure of the flame divided into zones of decisive influence*

Studies on reducing NO_x emissions are usually based on the structure of the flame in its entirety [5, 15, 27] with the separation of the flame nucleus and other parts thereof. The measures taken to reduce the intensity of NO_x formation anticipate the effect on the entire flame. Known methods for reducing NO_x emissions [4, 8-10, 30] developed on this basis include: humidifying the entire air stream in front of the burner or ballasting it with exhaust gases. Some achievements of such methods are indisputable but limited.

However, the majority of the currently produced burners are characterized by turbulent-diffusion combustion organization [2]. The flame in the burner tunnel and then in the furnace is not uniform. It consists of many individual and in some sense isolated structures. Each fuel stream, mixing with the air flowing into it, creates such a structure (in aerodynamic and thermodynamic terms). The combination of mutually building up structures constituting molar masses of burning fuel can be defined as mono-flame, micro-flame, partial or component flames. Each mono flame is a fairly determinate structure that reacts only with the surrounding air stream. In a simplified form, not taking into account the turbulence of flame. Figure 5 shows the aforementioned flame division zones and SDW-s occurring in each monoflow [16].

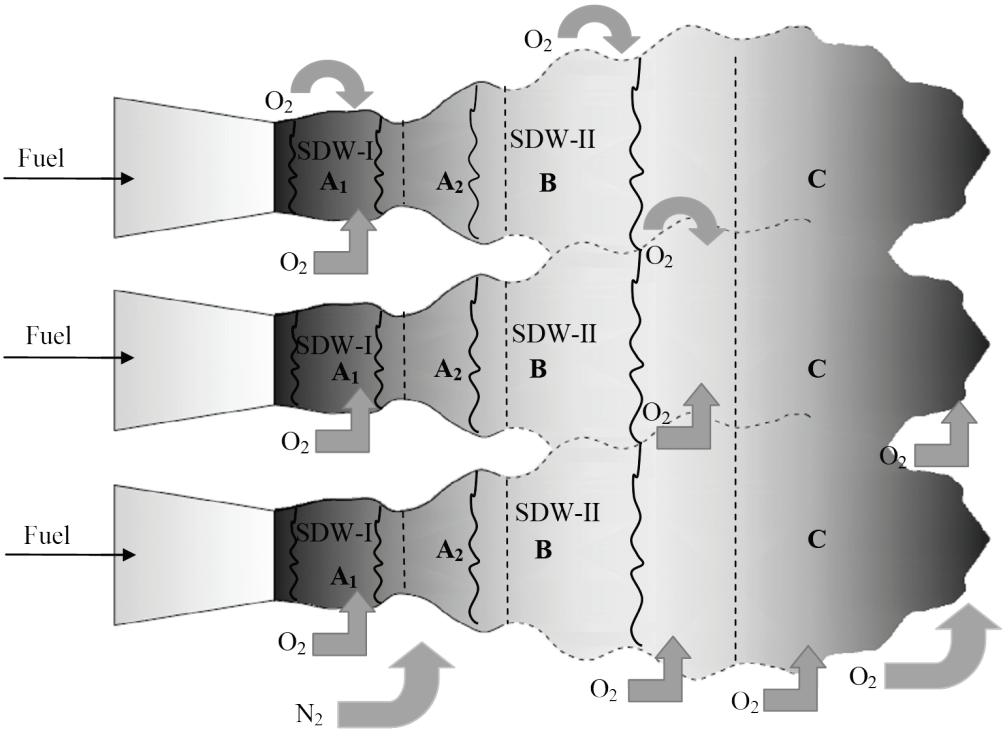

FIGURE 5. *Schematic diagram of the structure of a turbulent multi-stream flame*

The mono-flames retain their seclusion until the beginning of zone B. That is in zones SDW-I and SDW-II. The end of zone B and the entire zone C are characterized by a quick connection of mono-flames and the formation of a more uniform structure of the entire flame. From this point of view, the generally accepted principle of examining the flame in its entirety is contrary to the complex structure of the flame described above. The course of the processes of formation and combustion of nitrogen oxides in each mono-flame is somewhat independent. Based on the above premises, a method of impact on the SDW was proposed in each mono-flame. Experimental verification of these assumptions took place directly on steam boilers in operating boiler room conditions.

Research objects

The tests were carried out on four steam boilers of different power: DKVR 10-13, DKVR 20-13, DE 25-14 and PTVM-50. Each of the tested boilers was in a different industrial and heating boiler room located in the St. Petersburg district. All tested boilers operated on gaseous fuel. Characteristics of individual boilers are presented in Table 1.

TABLE 1. *List of boilers parameter values, on which investigations have been performed*

Parameter	Boiler type			
	DKVR10-13	**DKVR20-13**	**DE 25-14**	**PTVM-50**
Boiler heat power, MW	8.37	14.09	14.91	53.78
Type of burner	GMG-5.5	GMGB-5.6	GMP-16	DKZ
Number of burners	2	3	1	12
The fan and exhaust installation				
Blow fan	VD-8	VD-10	VD-10	WC-14-46-8
Exhaust fan	D-10	D-10	D-13.5	–

Based on the theoretical assumptions made above and the preliminary analysis of the flame structure by means of simulation and photography methods, individual constructions of moisture injection heads were developed for each boiler and burner. To ensure proper supply of water ballast to the SDW-I and SDW-II zones, the number of holes, their location and angle of inclination were subjected to each mono flame. During the tests, the pressure of injected steam was an additional factor. In the case of multi-burner boiler designs (i.e. PTVM-50 with 12 burners), parameters in different rows of burners were also differentiated. An example of such a head for the GMP-16 burner of the DE 25-14 boiler is shown in Figure 6. The design of the head provided intensive mechanical and chemical interaction in the SDW-I zone in the mono-flame of each gas stream. The rest of the water ballast provided interaction in SDW-II by dissociation of water vapor. This principle of active impact on SDW in each mono-flame has been referred to as directed dosed steam ballasting.

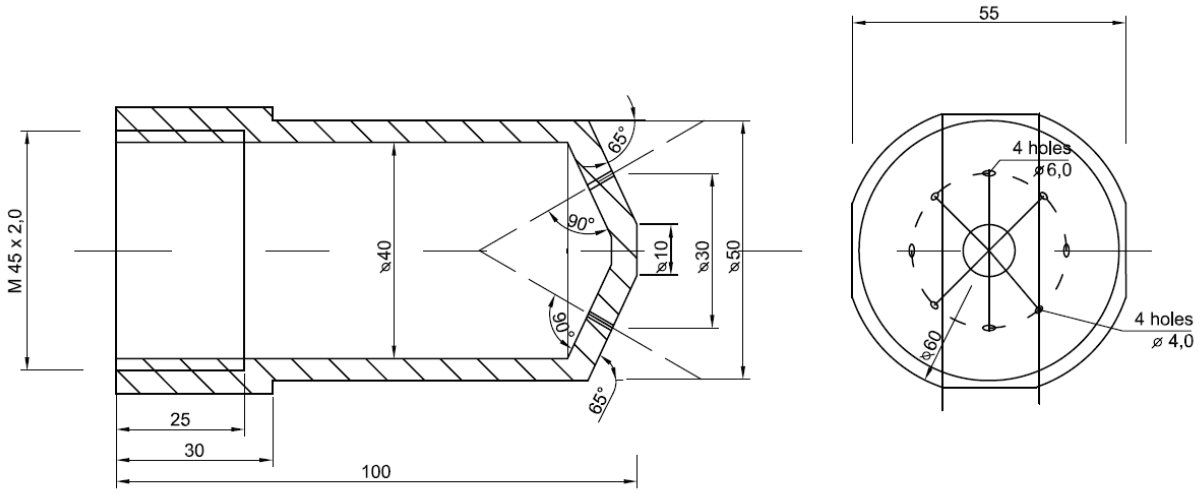

FIGURE 6. *Technical drawing of the exemplary design of the head for injecting moisture into the zones of decisive influence for the DE 25-14 boiler with the GMP-16 burner*

Experimental results

The investigations have been performed on four gas-fired boilers. The performed investigations allowed to achieve the best results of the use of the proposed method with an inject of the moisture into zones of decisive influence (SDW-I and SDW-II).

In Figure 7 the mass emission of nitrogen oxides as a function of boiler efficiency for two modes of its operation has been presented. The first mode relies on the measurements of mass emissions of nitrogen oxides during boiler work under its actual operating conditions, while the second one relies on the measurements with the additional suppression system of oxide emissions on [4]. In both cases, the value of the emission of nitrogen oxides depends on the boiler's steam capacity or its thermal power. The higher the steam output of the boiler or its heat output, the greater the mass emission of nitrogen oxides.

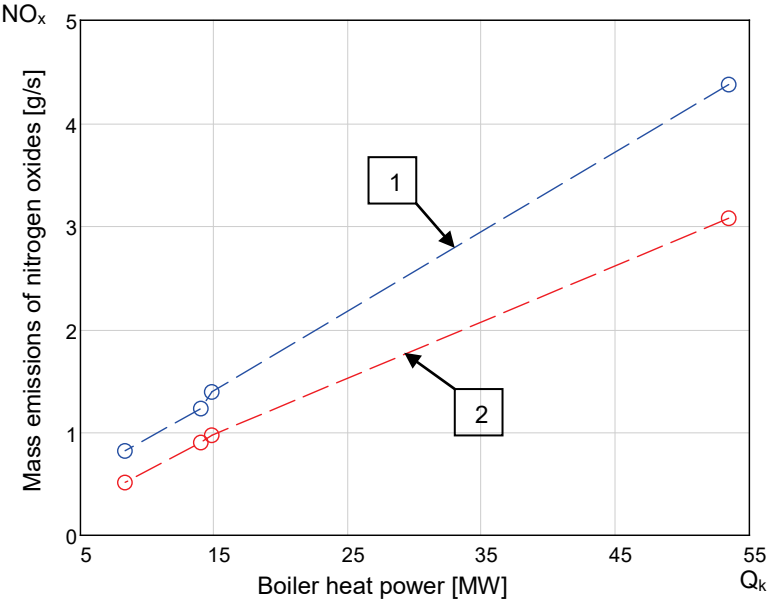

FIGURE 7. *The dependences of mass emission of nitrogen oxides as a function of boiler heat power (1 – boiler without additional systems activated, 2 – boiler with activated system of suppressing nitrogen oxides emission)*

In Figure 8 the obtained results of the mass value of nitrogen oxides emission, calculated to 1 MW heat power, for two boiler modes have been presented. This figure presents the effectiveness of the directed metered flame ballast method. The characteristics presents that the specific mass emissions

of nitrogen oxides are lower for boilers with maximum power with the system turned on than for boilers with the minimum power in normal operating modes (without the NO_x suppression system switched on). The application of an automatic suppression system of nitrogen oxides emission on each of the boilers allowed reducing this emission by average 30%. In the case of the DKVR 10-13 boiler, compared to the value obtained for actual operating conditions, the reduction in nitrogen oxide emissions reached 37%. The steam consumption per flame injection for each of the investigated boilers has been presented in Figure 9. In each case, the steam consumption per injection did not exceed 1% of the steam capacity of the boiler or its heat output. The increase of boiler efficiency, being a result of the use of the proposed method, compensated the steam consumption per injection.

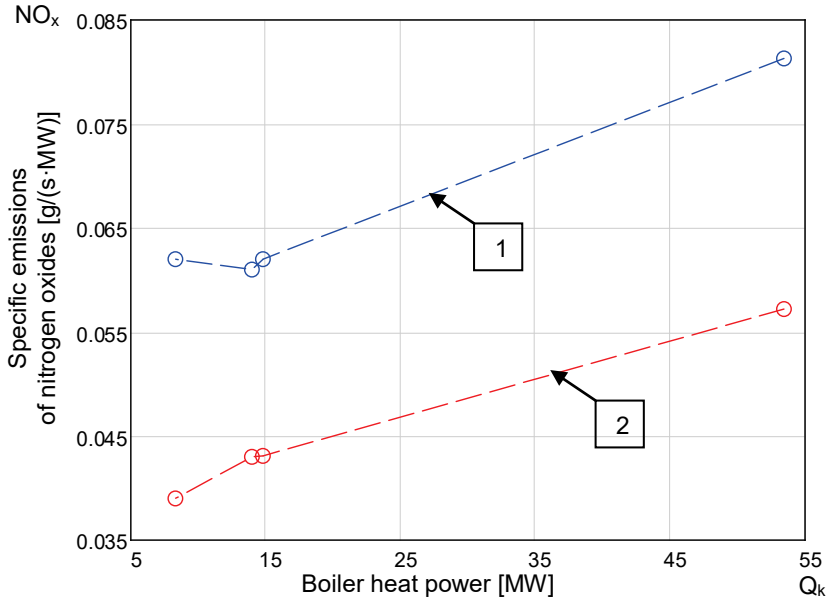

FIGURE 8. *Dependences of specific emissions of nitrogen oxides as a function of boiler heat power (1 – boiler without additional systems activated, 2 – boiler with activated system of suppressing nitrogen oxides emission)*

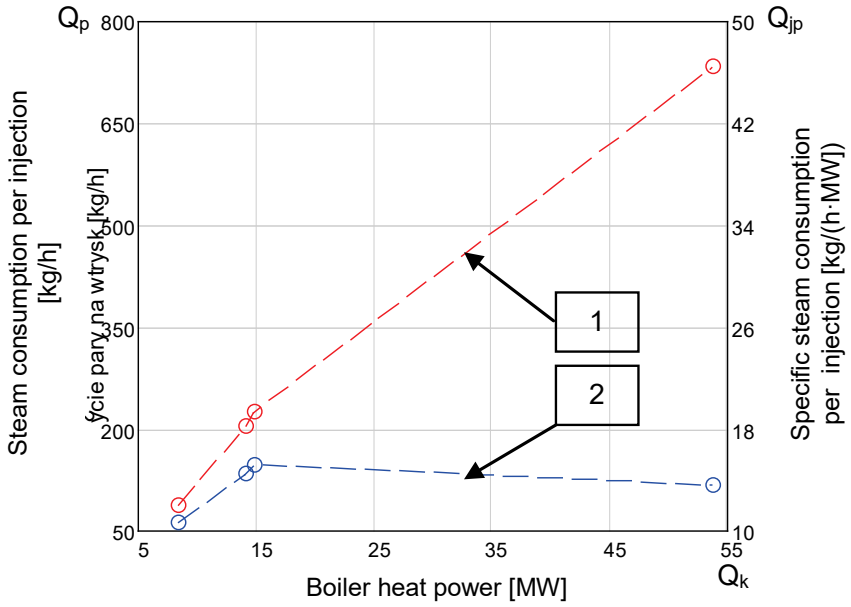

FIGURE 9. *The dependences of steam consumption (1 – absolute, 2 – unit) per injection as a function of boiler heat power (1 – absolute, 2 – unit)*

Conclusions

1. A method for reducing nitrogen oxide emissions in city heat boilers has been developed and proposed. The method relies in directing the dosed moisture injection into the flame zone.
2. The method has been experimentally verified on steam and water thermal power boilers with capacities from 8.37 to 53.79 MW. The number of the burners in these boilers was form 1 to 12.
3. It has been proved that the proposed method allows a reduction of nitrogen oxides by 30-40% with moisture injection not exceeding 0.9% of the boiler efficiency. Due the work of a boiler with moisture injection is accompanied by an increase in its efficiency to 1%, the use of the proposed method does not reduce the efficiency of fuel consumption in the heat source.

Conflicts of Interest: The author declares no conflict of interest.

REFERENCES

[1] Dal Secco S., Juan O., Louis-Louisy M., Lucas J.Y., Plion P., Porcheron L., *Using a genetic algorithm and CFD to identify low NO_x configurations in an industrial boiler*, Fuel, 158, 2015, pp. 672-683.

[2] Gradoń B., *Rola podtlenku azotu w modelowaniu emisji NO z procesów spalania paliw gazowych w piecach wysokotemperaturowych*, Zeszyty Naukowe Politechniki Śląskiej, Gliwice 2003.

[3] Herdzik J., Noch T., *Ballast Water Management Systems on Vessels. The Water Cleanliness Requirements of New D-2 Standard Versus the Expectations*, Rocznik Ochrona Środowiska, 20, 2018, pp. 647-661.

[4] Janta-Lipińska S., Shkarovskiy A., *The study on decreasing of nitrogen oxides emission carried out on DKVR 10-13 industrial heating boilers*, E3S Web of Conferences, 44, 2018.

[5] Jemieljanow A.A., *Development of injection devices to suppress nitrogen oxides when burning gas and mazout in boiler hearths*, Sankt Petersburg 1992.

[6] Kormilitsyn V.I., Ezhov V.S., *Studying the Removal of Nitrogen Oxides from Boiler Flue Gases in Firing Natural Gas*, Thermal Engineering, 60, 2, pp. 147-152.

[7] Konieczyński J., Komosiński B., Cieślik E., Konieczny T., Mathews B., Rachwał T., Rzońca G., *Research into Properties of Dust from Domestic Central Heating Boiler Fired with Coal and Solid Biofuels*, Archives of Environmental Protection, 43, 2, 2017, pp. 20-27.

[8] Krawczyk P., *Experimental investigation of N_2O formation in selective non-catalytic NO_x reduction processes performed in stoker boiler*, Polish Journal of Chemical Technology, 18, 4, 2016, pp. 104-109.

[9] Kuropka J., *Reduction of Nitrogen Oxides from Boiler Flue Gases*, Environment Protection Engineering, 36, 2, 2010, pp. 111-122.

[10] Lee C., Jou C.G., Tai H., Wang C., Hsieh S., Wang H.P., *Reduction of Nitrogen Oxide Emission of a Medium-Pressure Boiler by Fuel Control,* Aerosol and Air Quality Research, 6, 2, 2006, pp. 123-133.

[11] Man C.K., Gibbins J.R., Witkamp J.G., Zhang J., *Coal characterization for NO_x prediction in air-staged combustion of pulverised coals*, Fuel, 84, 17, 2005, pp. 2190-2195.

[12] Park H.Y., Baek S.H., Kim Y.J., Kim T.H., Kang D.S., Kim D.W., *Numerical and experimental investigations on the gas temperature deviation in a large scale, advanced low NO_x, tangentially fired pulverized coal boiler*, Fuel, 104, 2013, pp. 641-646.

[13] Pavlenko A., Szkarowski A., Janta-Lipińska S., *Research on Burning of Water Black Oil Emulsions*, Rocznik Ochrona Środowiska, 16, 2014, pp. 376-385.

[14] Shkarovskiy A.L., Novikov O.N., Novikova A.V., Polushhkin V.I., *Development of a new family of intelligent control systems of combustion quality*, Modern High Technologies, 12, 2016, pp. 556-561.

[15] Sigal I.J., *Air protection during fuel combustion*, Nedra, Leningrad 1988.

[16] Szkarowski A., *Principles of Calculation at Suppression of NO_x Formation by a Method of the Dosed Directed Injection of a Water Ballast*, Rocznik Ochrona Środowiska, 4, 2002, pp. 365-378.

[17] Szkarowski A., *Detailed Problems of the Effective and Ecologically Clean Combustion of Fuel in the Pre-grates of the Furnace*s, Rocznik Ochrona Środowiska, 5, 2003, pp. 67-78.

[18] Szkarowski A., Janta-Lipińska S., *Automatic Control of Burning Quality of Solid Fuel in Industrial Heating Boilers*, Rocznik Ochrona Środowiska, 11, 2009, pp. 241-255.

[19] Szkarowski A., Janta-Lipińska S., *Modeling of Optimum Burning of Fuel in Industrial Heating Boilers*, Rocznik Ochrona Środowiska, 13, 2011, pp. 511-524.

[20] Szkarowski A., Janta-Lipińska S., *Examination of Boiler Operation Energy-ecological Indicators During Fuel Burning with Controlled Residual Chemical Underburn*, Rocznik Ochrona Środowiska, 15, 2013, pp. 981-995.

[21] Szkarowski A., *Spalanie gazów. Teoria, praktyka, ekologia*, WNT, 2014.

[22] Szkarowski A., Janta-Lipińska S., *Experimental Research vs. Accuracy of the Elaborated Model*, Rocznik Ochrona Środowiska, 17, 2015, pp. 576-584.

[23] Szkarowski A., Janta-Lipińska S., Gawin R., *Reducing Emissions of Nitrogen Oxides from DKVR Boilers*, Rocznik Ochrona Środowiska, 18, 2016, pp. 565-578.

[24] Szkarowski A., Janta-Lipińska S., Dąbrowski T., *Research on Co-combustion of Gas and Oil Fuels*, Rocznik Ochrona Środowiska, 20, 2018, pp. 1515-1529.

[25] Szyszlak-Bargłowicz J., Zając G., Słowik T., *Hydrocarbon Emissions during Biomass Combustion*, Polish Journal of Environmental Studies, 24, 3, 2015, pp. 1349-1354.

[26] Szyszlak-Bargłowicz J., Zając G., Słowik T., *Research on Emissions from Combustion of Pellets in Agro Biomass Low Power Boiler*, Rocznik Ochrona Środowiska, 19, 2017, pp. 715-730.

[27] Tsyrulnikow L.M., *Methods for reducing the formation of toxic and corrosive combustion products of natural gas and fuel oil*, Overview information WNIIE Gazprom, series: The Most Important Scientific and Technical Problems of the Gas Industry, 1980.

[28] Wilk M., Magdziarz A., Kuźnia M., Jerzak W., *The reduction of the emission of NO_x in the heat-treating furnaces*, Metallurgy and Foundry Engineering, 36, 2010, pp. 47-54.

[29] Xu H., Smoot L.D., Hill S.C., *Computational model for NO_x reduction by advanced reburning*, Energy & Fuels, 13, 2, 1999, pp. 411-420.

[30] Xue S., Hui S.E., Liu T.S., Zhou Q.L., Xu T.M., Hu H.L., *Experimental investigation on NO_x emission and carbon burnout from a radially biased pulverized coal whirl burner*, Fuel Processing Technology, 90, 9, 2009, pp. 1142-1147.

[31] Zając G., Szyszlak-Bargłowicz J., Słowik T., Wasilewski J., Kuranc A., *Emission Characteristics of Biomass Combustion in a Domestic Heating Boiler Fed with Wood and Virginia Mallow Pellets*, Fresenius Environmental Bulletin, 26, 7, 2017, pp. 4663-4670.

[32] Zandeckis A., Blumberga D., Rochas C., Veidenbergs I., Silins K., *Methods of Nitrogen Oxide Reduction in Pellet Boilers*, Scientific Journal of RTU, Environmental and Climate Technologies, 4, 2010, pp. 123-129.

[33] Zeldovich J., *The oxidation of nitrogen in combustion and explosions*, European Physical Journal A. Hadrons and Nuclei, 21, 1946, pp. 577-628.

[34] Zhang X., Zhou J., Sun S., Sun R., Qin M., *Numerical investigation of low NO_x combustion strategies in tangentially-fired coal boilers*, Fuel, 142, 2015, pp. 215-221.

Roman M. RADCHENKO[1]
Dariusz MIKIELEWICZ[2]
Mykola I. RADCHENKO[1]
Victoria S. KORNIENKO[1]
Andrii A. ANDREEV[1]
Maxim A. PYRYSUNKO[1]

[1] *Admiral Makarov National University of Shipbuilding, 9 Heroes of Ukraine Avenue, Mykolayiv, Ukraine*

[2] *Gdańsk University of Technology 11/12 Gabriela Narutowicza Street, 80-233 Gdansk, Poland*

DOI: 10.53412/jntes-2020-3.3

MAIN ENGINE OF TRANSPORT SHIP INLET AIR COOLING BY EJECTOR CHILLER

Abstract: *The efficiency of cooling the air at the inlet of marine slow speed diesel engine turbocharger by ejector chiller utilizing the heat of exhaust gases and scavenge air were analyzed. The values of air temperature drop at the inlet of engine turbocharger and corresponding decrease in fuel consumption of the engine at varying climatic conditions on the route line Odessa–Yokohama–Odessa were evaluated.*

Keywords: *internal combustion engine, ejector chiller.*

Introduction

Slow speed diesel engines are the most widespread as the main engines of the ships. The fuel efficiency of diesel engines are considerable effected by the variations in ambient air temperatures along the route lines [1, 2]. The increase in marine low speed diesel engines intake air temperature by 10°C causes specific fuel consumption increase by 1.1 g/(kWh) to 1.2 g/(kWh) [3, 4].

In order to enhance the fuel efficiency of the engine it is necessary to cool the cyclic air: at the intake of turbocharger and scavenge air after turbocharger [5, 6]. Waste heat recovery chillers can be applied for engine air cooling [7, 8].

The absorption lithium-bromide chillers (ACh) are the most used for cooling air to about 15°C with a high coefficient of performance COP of 0.7 to 0.8 [9, 10]. But large sizes make mounting the ACh unit in engine room problematical. The ECh consist of heat exchangers [11, 12] suitable for mounting in free spaces. They enables deep cooling air but with a low COP of 0.2 to 0.35 [13, 14] and suitable for transport applications [15, 16].

The heat loss with exhaust gases represents a high part of the total waste heat in combustion engines [17, 18]. The low-temperature economizers [19, 20] use a condensation heat of sulfuric acid and water vapors. The condensed acid vapor glues the ash in exhaust gas, and adheres on heating surface [21], that increases the hydraulic and thermal resistance [22]. The experience of using WFE in boilers and diesel engines indicates the undeniable advantages of this type of fuel: the effective specific fuel consumption decreases by about 8% [23], the concentration of nitrogen oxides in exhaust gases is reduced in 1.4 to 3.1 times [24], CO – in 1.3 to 1.5 times [25], smoke – in 1.3 to 2.4 times [26]. The analysis of literary sources shows, that there is no quantitative data on low-temperature corrosion (LTC) intensity on condensation low-temperature heating surfaces (LTHS) of EGB while WFE combustion.

A double effect is achieved with WFE combustion: enhanced fragmentation of WFE droplets due to their microexplosions intensifies the combustion processes and reduces the particle emission as result, as well as intensifies entrainment of small particles by the exhaust gas flow and decreases their deposits on condensing/heating economizer surfaces and their thermal resistance as result [27, 28].

The purpose of the work is to estimate the efficiency of cooling the intake air of marine slow speed diesel engine by ejector chiller taking into account the variable climatic conditions along the route line.

Methodology

A slow speed diesel engine 6S60MC6.1-TI [2] is considered as an example of the main engine of transport vessel: nominal power N_n = 12.24 MW and continuous service power N_s = 10 MW. For the 6S60MC6.1-TI engine, according to the data of the MAN company (according to the calculations by using "mandieselturbo" software package), cooling inlet air for every 1°C results in reduction of specific fuel consumption within 0.11 g/(kWh) to 0.12 g/(kWh) [2-4].

The efficiency of engine intake air cooling is estimated by decrease in specific fuel consumption Δb_e due to reduce of intake air temperature Δt_a, that depends on the heat Q_h extracted from the exhaust gas and scavenge air and the efficiency of its conversion in refrigeration capacity Q_0 of the chiller, i.e. coefficient of performance COP.

The efficiency of conversion of waste heat into refrigeration capacity is characterized by coefficient of performance $\zeta = Q_0 / Q_h$ as the ratio of the chiller refrigeration capacity Q_0 to the consumed heat Q_h, extracted from the engine exhaust gases, scavenge air and others.

The available refrigeration capacity Q_0 of ECh is calculated as $Q_{0.\text{ECh}} = Q_h \zeta_{\text{ECh}}$, where Q_h is the heat, extracted from the engine exhaust gases and scavenge.

The values of the available air temperature drop in the ECh air cooler $\Delta t_{a.\text{ECh}}$ due to using ECh available refrigeration capacities $Q_{0.\text{ECh}} = Q_h \zeta_{\text{ECh}}$ is calculated proceeding from the heat balance $Q_{0.\text{ECh}} = G_a \xi_a c_a \Delta t_{a.\text{ECh}}$ as $\Delta t_a = Q_{0.\text{ECh}} / G_a \xi_a c_a$, where: G_a – air mass flow rate, kg/s; c_a – specific heat capacity of wet air, kW/(kg·K); ξ_a – specific heat ratio of cooling air process in air cooler.

The available temperatures of cooled air at the outlet of the air cooler $t_{a2} = t_{a1} - \Delta t_a$.

The current values of reduction in specific fuel consumption per 1 hour: $\Delta b_e = \Delta t_a \cdot \Delta b_{e1°\text{C}}$, g/kWh, and the total fuel reduction per 1 hour: $\Delta B_e = N_s \Delta b_e$ or $\Delta B_e = N_s \Delta t_a \Delta b_{e1°\text{C}}$, g/h, where: $\Delta b_{e1°\text{C}}$ – reduction in specific fuel consumption referred to engine intake air temperature drop in 1°C or 1 K, $\Delta b_{e1°\text{C}} = \Delta b_e / \Delta t_a$ = 0.12 g/(kWh·K); N_s = 10000 kW – diesel engine power output.

A refrigeration capacity of ejector chiller Q_0 is defined from available exhaust gas heat Q_G as $Q_0 = \zeta Q_G$, where ζ is coefficient of performance of ejector chiller, ζ = 0.35.

Results

A schema of developed engine intake air cooling system with ejector chiller utilizing the heat of exhaust gas is shown in Figure 1.

The ejector chiller consists of power and refrigeration contours. A generator of power contour uses a heat of exhaust gas to produce a high pressure refrigerant vapour as a motive fluid which energy is used in ejector to compress the low pressure refrigerant vapour, sucked from evaporator-intake air cooler of refrigeration contour, up to the pressure in the condenser.

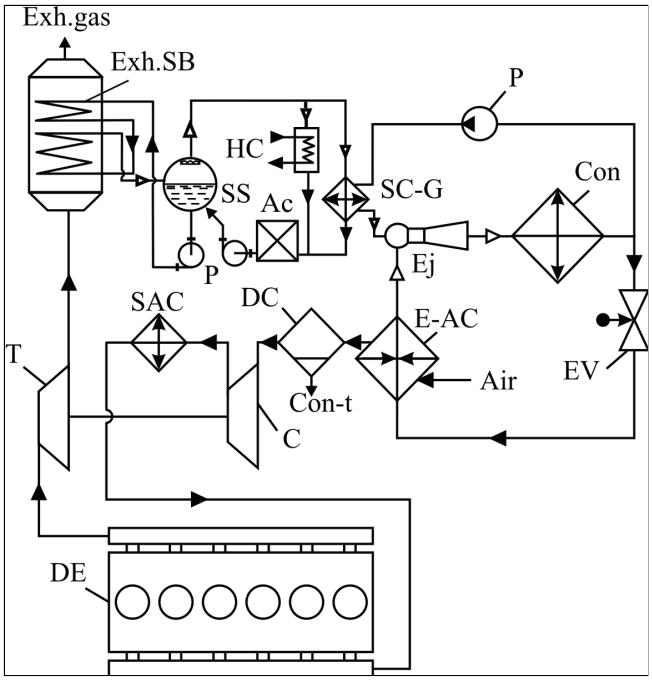

FIGURE 1. *Schema of the engine intake air cooling system with ejector chiller utilizing the heat of exhaust gas: DE – diesel engine, T – turbine and C – compressor of turbocharger, SAC – scavenge air cooler, Exh.SB – exhaust gas steam boiler (economizer), SC-G – steam condenser-generator of refrigerant vapour, E-AC – evaporator-air cooler, Ej – ejector, Con – condenser, EV – expansion valve, P – pump, Con-t – condensate of water steam, DC – droplet catcher, Ac – accumulator of feed water, SS – steam separator, HC – heat consumer*

The efficiency of application of ejector chiller (ECh) for cooling engine intake air is estimated by decrease in specific fuel consumption Δb_e of diesel engine due to reduction of intake air temperature Δt_a, that depends on the heat extracted from the exhaust gas (heat load on the generator of ejector chiller) and the efficiency of its conversion in refrigeration capacity (refrigeration capacity of the ejector chiller (heat removed from intake air in refrigerant evaporator-air cooler), i.e. coefficient of performance COP.

A route line Odessa–Yokohama–Odessa (June-July) 2019 is considered (Fig. 2).

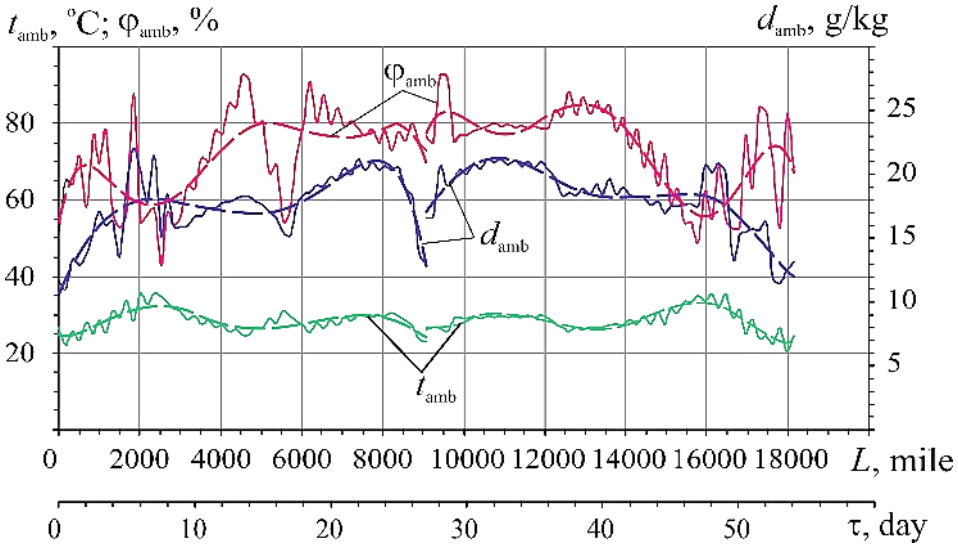

FIGURE 2. *Variation of ambient air temperature t_{amb}, relative humidity φ_{amb} and absolute humidity d_{amb} on the route line Odessa–Yokohama–Odessa*

For each time interval (3 hours) along the route line Odessa–Yokohama–Odessa the values of ambient air temperature t_{amb} and relative humidity φ_{amb} were fixed by applying the well-known program "mundomanz.com" to calculate the processes of cooling intake air in the air cooler at the inlet of

turbocharger of diesel engine and define the required temperature drops Δt_a and refrigeration capacities $Q_{0.\text{ECh}}$, as well as the available air temperature drop in the ECh air cooler Δt_a due to using the available refrigeration capacities $Q_{0.\text{ECh}}$ of ECh utilizing the heat of engine exhaust gas and scavenge air.

A decrease in the temperature of air Δt_a at the inlet of engine turbocharger due to its cooling by ejector chiller and, accordingly, the effect of its application depends on the heat of steam produced by exhaust steam boiler (ExhSB), that remains after covering all the ship heat demands. During warm time steam consumption on the bulk carrier is approximately 25% of steam productivity of exhaust boiler, i.e. 75% of steam produced can be used in ejector chiller for cooling the engine turbocharger intake air.

Besides, decrease in temperature of air in the air cooler at the inlet of diesel engine turbocharger $\Delta t_a = t_{a1} - t_{a2}$ depends on temperature t_{a1} and relative humidity φ_a of intake air in the engine room, in turn, depending on parameters of ambient air, i.e. sailing environmental conditions. During sailing in warm time the air temperature in the engine room t_{ER} exceeds ambient temperature by 10°C [1].

The temperature t_{a2}, which limits the depth of engine intake air cooling in the air cooler, in turn, depends on the temperature of boiling refrigerant. A temperature of boiling refrigerant R142b in the evaporator-air cooler is desirable about t_0 = 7°C. The temperature difference between cooled air and boiling refrigerant can be accepted 8°C. Taking into account these values a depth of cooling the air in the evaporator-air cooler is limited to minimum temperature $t_{a2} = t_0 + 8 = 15$°C.

For each time interval (3 hours) and corresponding temperature t_{amb} and relative humidity φ_{amb} of ambient air the processes of cooling of intake air in the air cooler at the inlet of turbocharger of diesel engine, from the air temperature at the cooler inlet (in engine room) $t_{a1} = t_{amb} + 10$°C to air cooler outlet air temperature t_{a2} have been calculated.

Values of air temperature drop in the air cooler of ejector chiller, utilizing a heat of exhaust gas (schema in Fig. 1), Δt_a, are presented in Figure 3.

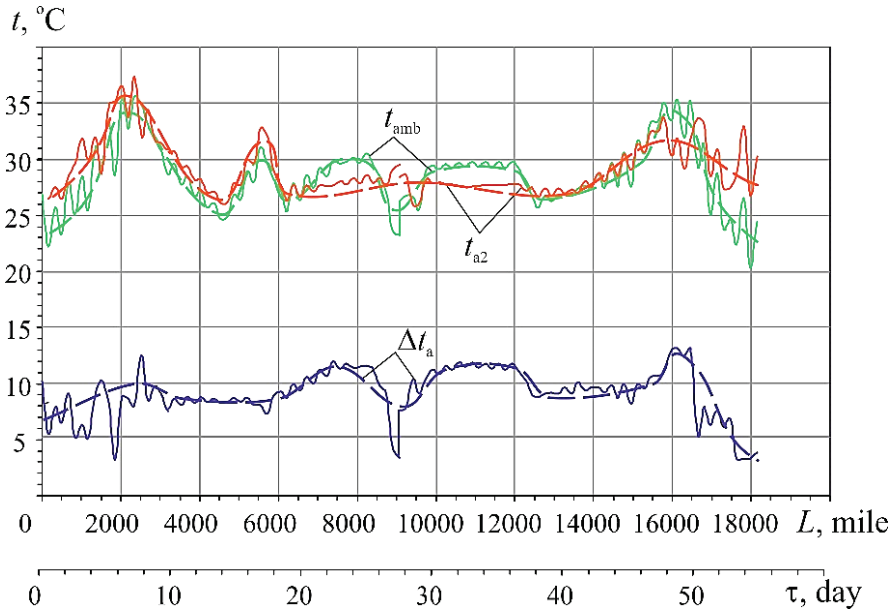

FIGURE 3. *Air temperature drops Δt_a in the air cooler of ECh according to available ECh refrigeration capacities Q_0 due to utilizing a heat of exhaust gas and corresponding temperatures of cooled air at the outlet of air coolers t_{a2} with variation of ambient air temperature t_{amb} on the route line Odessa–Yokohama–Odessa (June-July, 2019)*

As it is shown, decrease in temperature of air in the air cooler of ejector chiller, utilizing a heat of exhaust gas (Fig. 1) Δt_a = 13°C, ..., 18°C. In the case of using only exhaust gas heat a decrease in temperature of air in the air cooler of ejector chiller Δt_a is not enough for lowering air temperature to

the minimum value (15°C), which might be possible at refrigerant boiling temperature in the air cooler t_0 = 7°C: temperature t_{a2} at the exit of air cooler is sometimes higher then 15°C (Fig. 3).

Relative values $\Delta Q_0^{''}$ ΔQ_0 of refrigeration capacities required (needed for engine intake air cooling to t_{a2} = 15°C) referred to available ECh refrigeration capacities due to utilizing a heat of exhaust gas are shown in Figure 4.

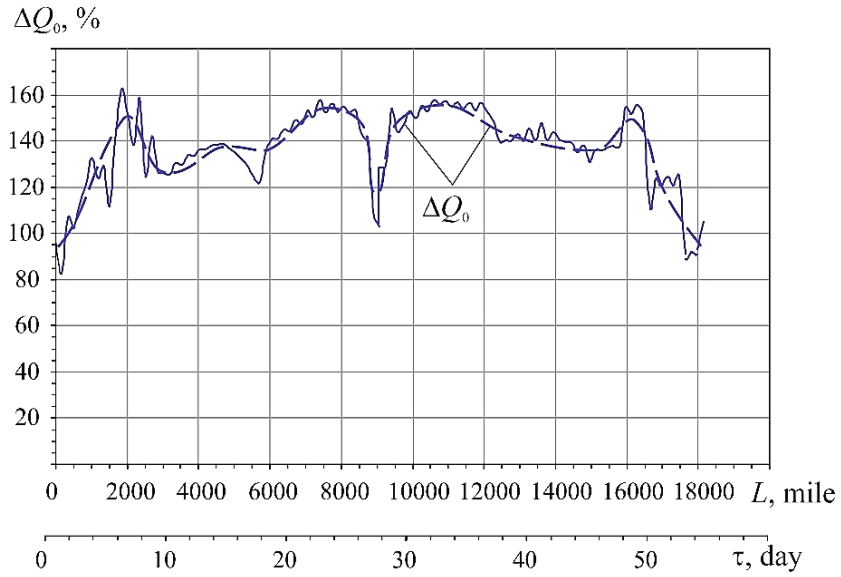

FIGURE 4. *Relative values ΔQ_0 of refrigeration capacities needed for engine intake air cooling to t_{a2} = 15°C referred to available ECh refrigeration capacities due to utilizing a heat of exhaust gas*

As the relative values $\Delta Q_0 \Delta Q_0^{''}$ of refrigeration capacities needed for engine intake air cooling to t_{a2} = 15°C referred to available ECh refrigeration capacities show, the refrigeration capacities needed for engine intake air cooling to t_{a2} = 15°C considerable exceed the available ECh refrigeration capacities by 40%, …, 50% when the only exhaust gas heat is used: $\Delta Q_0^{''}$ = 140%, …, 150% (Fig. 4).

Decrease in specific fuel consumption Δb_e of diesel engine, fuel reduction in absolute B_e, t, and relative $B_e^{'}$, %, values on the route line Odessa–Yokohama–Odessa due to cooling intake air by ejector chiller, using exhaust gas heat (Fig. 1), calculated by program "mandieselturbo" [2], are shown in Figure 5.

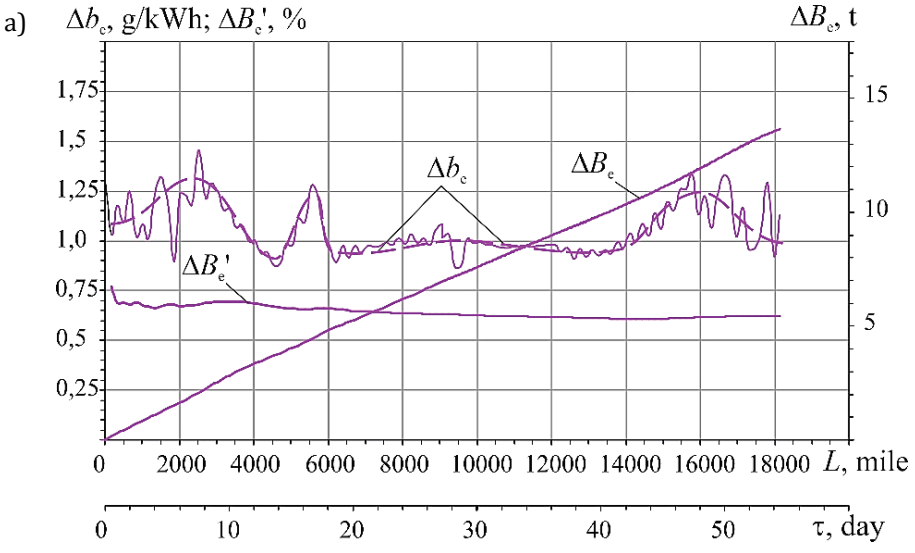

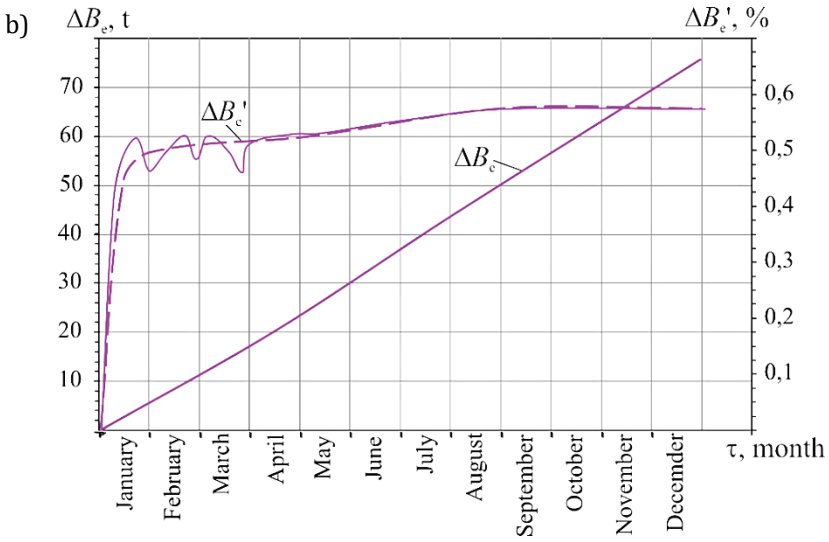

FIGURE 5. *Decrease of specific fuel consumption Δb_e, total fuel consumption for engine power N_s = 10000 kW in absolute ΔB_e, t and relative $\Delta B_e'$, %, values referred to the engine total fuel consumption due to cooling intake air by ejector chiller, using exhaust gas heat on the route line Odessa–Yokohama–Odessa, June-July 2019 (a) and their summarized annual absolute ΔB_e and relative $\Delta B_e'$ values on the route line Odessa–Yokohama–Odessa in 2019 (b)*

As Figure 5 shows, a decrease of specific fuel consumption due to intake air cooling by ejector chiller Δb_e = 1.0 g/(kW·h), …, 1.2 g/(kW·h), absolute fuel saving during the routes Odessa–Yokohama–Odessa, June-July 2019, is ΔB_e = 13 t (Fig. 5a) and annual fuel saving ΔB_e = 75 t (Fig. 5b) and the relative fuel saving $\Delta B_e'$ is a bit higher than 0.6% for diesel engine 6S60MC6.1-TI (continuous service power N_s = 10 MW).

In order to provide a deeper engine intake air cooling for the operation of engine at the temperature t_{a2} of about 15°C it is necessary to use addition heat, for instance scavenge air heat.

A schema of developed engine intake air cooling system with ejector chiller utilizing the heat of exhaust gas in evaporative section of ECh generator and scavenge air in economizer section is shown in Figure 6.

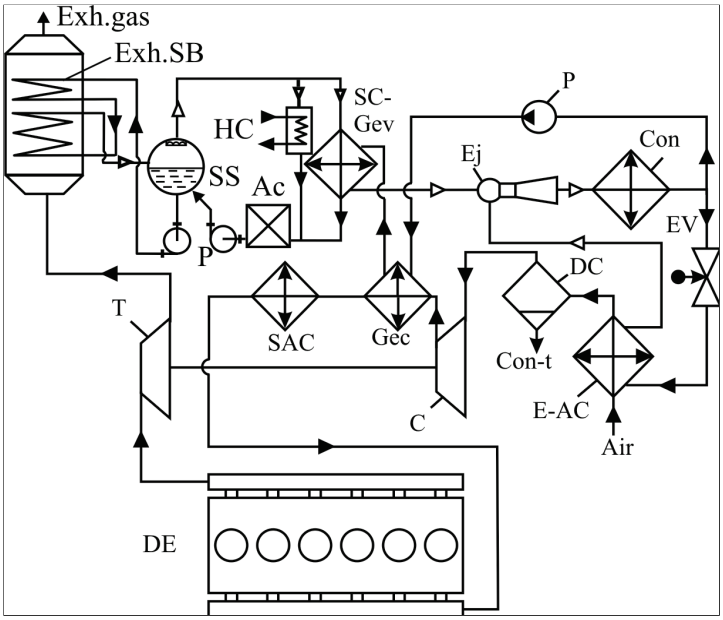

FIGURE 6. *A schema of the engine intake air cooling system with ejector chiller utilizing the heat of exhaust gas and scavenge air: DE – diesel engine, T – turbine, C – compressor of turbocharger, SAC – scavenge air cooler, Exh.SB – exhaust gas steam boiler, SC-Gev – steam condenser-evaporative section of ECh generator, Gec – economizer section of ECh generator, E-AC – evaporator-air cooler, Ej – ejector, Con – condenser, EV – expansion valve, P – pump, Con-t – condensate, DC – droplet catcher, Ac – accumulator of feed water, SS – steam separator, HC – heat consumer*

The ejector chiller consists of power and refrigeration contours. A generator of power contour uses a heat of exhaust gas to produce a high pressure refrigerant vapour as a motive fluid which energy is used in ejector to compress the low pressure refrigerant vapour, sucked from evaporator-intake air cooler of refrigeration contour, up to the pressure in the condenser.

Values of air temperature drop in the air cooler of ejector chiller, utilizing a heat of exhaust gas and scavenge air (Fig. 6), Δt_a, are presented in Figure 7.

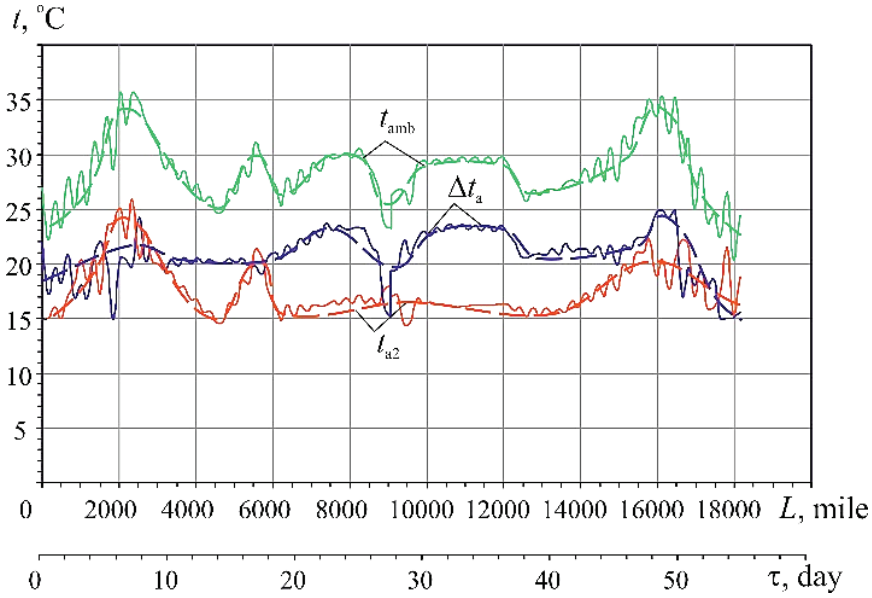

FIGURE 7. *Air temperature drops Δt_a in the air cooler of ECh according to available ECh refrigeration capacities Q_0 due to utilizing a heat of exhaust gas and corresponding temperatures of cooled air at the outlet of air coolers t_{a2} with variation of ambient air temperature t_{amb} on the route line Odessa–Yokohama–Odessa (June-July, 2019)*

As it is shown, decrease in temperature of air in the air cooler of ejector chiller, utilizing a heat of exhaust gas and scavenge air (Fig. 6) Δt_a = 20°C, ..., 23°C (Fig. 7).

Relative values ΔQ_0 of refrigeration capacities needed for engine intake air cooling to t_{a2} = 15°C referred to available ECh refrigeration capacities due to utilizing a heat of exhaust gas and scavenge air are presented in Figure 8.

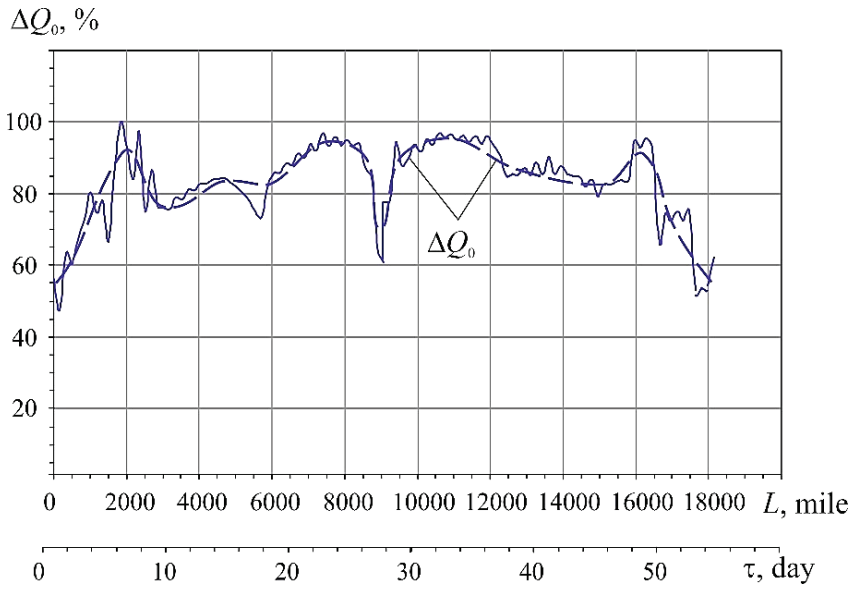

FIGURE 8. *Relative values ΔQ_0 ($\Delta Q_0'$) of refrigeration capacities needed for engine intake air cooling to t_{a2} = 15°C referred to available ECh refrigeration capacities due to utilizing the heat of exhaust gas and scavenge air*

As Figure 8 shows, the relative values ΔQ_0 (ΔQ_0') of refrigeration capacities needed for engine intake air cooling to t_{a2} = 15°C are generally less than 100%, that means that the available ECh refrigeration capacities while utilizing the heat of exhaust gas and scavenge air are generally enaugh for cooling diesel engine intake air to t_{a2} = 15°C.

The results of calculations of fuel saving due to cooling diesel engine intake air by ejector chiller, using exhaust gas and scavenge air heat on the route line Odessa–Yokohama–Odessa, June-July 2019 and their summarized annual (Fig. 6), calculated by program "mandieselturbo", are shown in Figure 9.

Decrease in specific fuel consumption Δb_e, g/(kW·h), of diesel engine, fuel saving in absolute B_e, t, and relative B_e', %, values on the route line Odessa–Yokohama–Odessa and their summarized annual absolute ΔB_e and relative $\Delta B_e'$ values due to cooling intake air by ejector chiller, using exhaust gas and scavenge air heat are resulted in Figure 9.

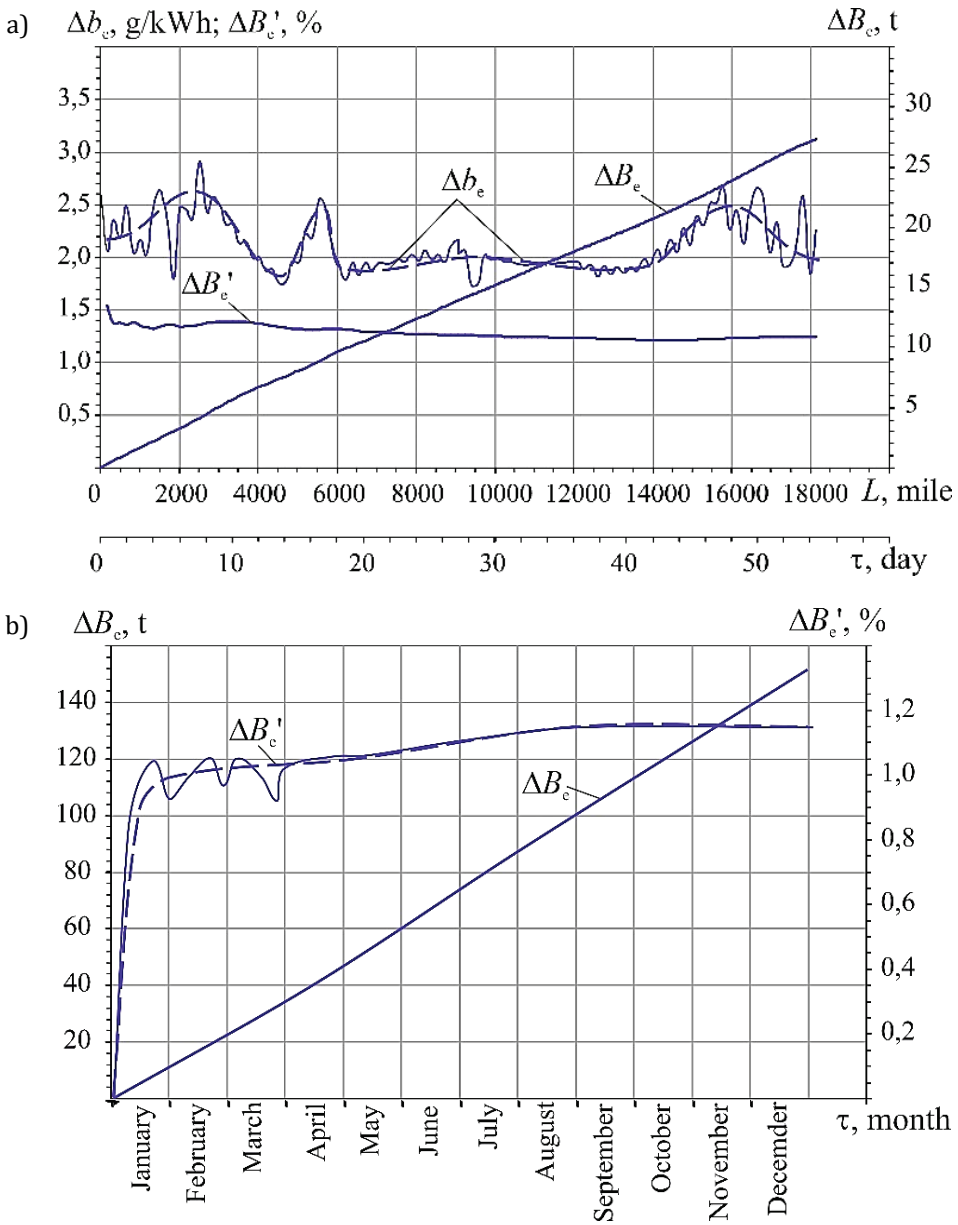

FIGURE 9. *Decrease of specific fuel consumption Δb_e, total fuel consumption for engine power N_s = 10000 kW in absolute ΔB_e, t, and relative $\Delta B_e'$, %, values referred to the engine total fuel consumption on the route line Odessa–Yokohama–Odessa, June-July 2019 (a) and their summarized annual absolute ΔB_e and relative $\Delta B_e'$ values (b)*

As Figure 9 shows, a decrease of specific fuel consumption due to intake air cooling by ejector chiller Δb_e = 2.0 g/(kW·h), …, 2.5 g/(kW·h), absolute fuel saving during the routes Odessa–Yokohama–Odessa, June-July 2019, is ΔB_e = 26 t (Fig. 9a) and annual fuel saving ΔB_e = 150 t (Fig. 9b) and the relative fuel saving $\Delta B_e^{'}$ is about 1.3% for diesel engine 6S60MC6.1-TI (continuous service power N_s = 10 MW).

In order to provide a deeper engine intake air cooling to the temperature t_{a2} of about 10°C and lower it is necessary to apply two-stage cooling air in hybrid water-refrigerant air cooler by combined absorption-ejector chillers with higher COP.

Conclusions

The efficiency of application of waste heat recovery ejector chiller system for cooling the intake air of marine diesel engine has been analyzed for real changeable climatic conditions on the routes Odessa–Yokohama–Odessa.

The application of ejector chiller provides reducing the engine intake air temperature by 20°C, …, 23°C with corresponding decrease of specific fuel consumption by 2.0 g/(kWh), …, 2.5 g/(kWh).

In order to provide a deeper engine intake air cooling to the temperature t_{a2} of about 10°C and lower it is necessary to apply two-stage cooling air in a hybrid water-refrigerant air cooler by combined absorption-ejector chillers with a higher COP.

Conflicts of Interest: The author declares no conflict of interest.

REFERENCES

[1] MAN B&W ME/ME-C/ME-GI/ME-B-TII engines, MAN Diesel, Copenhagen, Denmark 2010, p. 389.

[2] Wärtsilä Environmental Product Guide, online, available at: https://cdn.wartsila.com/docs/default-source/product-files/egc/product-guide-o-env-environmental-solutions.pdf (April 2017).

[3] MAN Diesel Turbo, CEAS Engine Calculations, online, 2019, available at: https://marine.man-es.com/two-stroke/ceas.

[4] MAN Diesel & Turbo, MAN B&W Two-stroke Marine Engines. Emission Project Guide, online, available at: https://marine.man-es.com/applications/projectguides/2stroke/content/special_pg/7020-0145-09_uk.pdf (accessed 9 October 2018).

[5] Radchenko A., Mikielewicz D., Forduy S., Radchenko M., Zubarev A., *Monitoring the fuel efficiency of gas engine in integrated energy system* [in:] Nechyporuk M. et al. (eds.), ICTM 2019, AISC, Springer, Vol. 1113, Cham 2020, pp. 361-370.

[6] Radchenko R., Kornienko V., Pyrysunko M., Bogdanov M., Andreev A., *Enhancing the efficiency of marine diesel engine by deep waste heat recovery on the base of its simulation along the route line* [in:] Nechyporuk M. et al. (eds.), ICTME, AISC, Springer, Vol. 1113, Cham 2020, pp. 337-350.

[7] Radchenko A., Stachel A., Forduy S., Portnoi B., Rizun O., *Analysis of the efficiency of engine inlet air chilling unit with cooling towers* [in:] Ivanov V. et al. (eds.), ADSM III (DSMIE 2020), LNME, Springer, Cham 2020, pp. 322-331.

[8] Konovalov D., Kobalava H., Radchenko M., Scurtu I.C., Radchenko R., *Determination of hydraulic resistance of the aerothermopressor for gas turbine cyclic air cooling* [in:] TE-RE-RD 2020, E3S Web of Conferences, Vol. 180, 2020, No. 01012.

[9] Radchenko A., Trushliakov E., Kosowski K., Mikielewicz D., Radchenko M., *Innovative turbine intake air cooling systems and their rational designing*, Energies, 2020, Vol. 13, Issue 23, No. 6201.

[10] Trushliakov E., Radchenko A., Forduy S., Zubarev A., Hrych A., *Increasing the operation efficiency of air conditioning system for integrated power plant on the base of its monitoring* [in:] Nechyporuk M. et al. (eds.), ICTME (ICTM 2019), AISC, Springer, Vol. 1113, Cham 2020, pp. 351-360.

[11] Butrymowicz D., Gagan J., Śmierciew K., Łukaszuk M., Dudar A., Pawluczuk A., Łapiński A., Kuryłowic A., *Investigations of prototype ejection refrigeration system driven by low grade heat*, HTRSE-2018, E3S Web of Conferences 2018, Vol. 70, p. 7.

[12] Forduy S., Radchenko A., Kuczynski W., Zubarev A., Konovalov D., *Enhancing the fuel efficiency of gas engines in integrated energy system by chilling cyclic air* [in:] Tonkonogyi V. et al. (eds.), Grabchenko's ICAMP, InterPartner-2019, LNME, Springer, Cham 2020, pp. 500-509.

[13] Radchenko R., Pyrysunko M., Radchenko A., Andreev A., Kornienko V., *Ship engine intake air cooling by ejector chiller using recirculation gas heat* [in:] Tonkonogyi V. et al. (eds.), AMP. InterPartner-2020, LNME, Springer, Cham 2021, pp. 734-743.

[14] Radchenko M., Radchenko R., Tkachenko V., Kantor S., Smolyanoy E., *Increasing the operation efficiency of railway air conditioning system on the base of its simulation along the route line* [in:] Nechyporuk M. et al. (eds.), ICTME (ICTM 2019), AISC, Springer, Vol. 1113, Cham 2020, pp. 461-467.

[15] Trushliakov E., Radchenko M., Bohdal T., Radchenko R., Kantor S., *An innovative air conditioning system for changeable heat loads* [in:] Tonkonogyi V. et al. (eds.), ICAMP, InterPartner-2019, LNME, Springer, Cham 2020, pp. 616-625.

[16] Trushliakov E., Radchenko A., Radchenko M., Kantor S., Zielikov O., *The Efficiency of refrigeration capacity regulation in the ambient air conditioning systems* [in:] Ivanov V. et al. (eds.), Advances in Design, Simulation and Manufacturing III (DSMIE 2020), LNME, Springer, Cham 2020, pp. 343-353.

[17] Luo C., Luo K., Wang Y., Ma Z., Gong Y., *The effect analysis of thermal efficiency and optimal design for boiler system*, Energy Procedia, Vol. 105, 2017, pp. 3045-3050.

[18] Syed Safeer Mehdi Shamsi, Assmelash A. Negash, Gyu Baek Cho, Young Min Kim, *Waste heat and water recovery system optimization for flue gas in thermal power plants*, Sustainability, Vol. 11, Issue 7, No. 1881, 2019.

[19] Kornienko V., Radchenko M., Radchenko R., Konovalov D., Andreev A., Pyrysunko M., *Improving the efficiency of heat recovery circuits of cogeneration plants with combustion of water-fuel emulsions*, Thermal Science, Vol. 25, Issue 1, Part B, 2021, pp. 791-800.

[20] Baldi S., Quang T.L., Holub O., Endel P., *Real-time monitoring energy efficiency and performance degradation of condensing boilers*, Energy Conversion and Management, Vol. 136, 2017, pp. 329-339.

[21] Fan C., Pei D., Wei H., *A novel cascade energy utilization to improve efficiency of double reheat cycle*, Energy Convers. Manag., Vol. 171, 2018, pp. 1388-1396.

[22] Sugeng D.A., Ithnin A.M., Amri N.S.M.S., Ahmad M.A., Yahya W.J., *Water content determination of steam generated water-in-diesel emulsion*, Journal of Advanced Research in Fluid Mechanics and Thermal Sciences, Vol. 49, Issue 1, pp. 62-68.

[23] Baskar P., Senthil Kumar A., *Experimental investigation on performance characteristics of a diesel engine using diesel-water emulsion with oxygen enriched air*, Alexandria Engineering Journal, Vol. 56, Issue 1, 2017, pp. 137-146.

[24] Patel K.R., Dhiman V., *Research study of water- diesel emulsion as alternative fuel in diesel engine – An overview*, International Journal of Latest Engineering Research and Applications, Vol. 2, Issue 9, 2017, pp. 37-41.

[25] Wojs M.K., Orliński P., Kamela W., Kruczyński P., *Research on the influence of ozone dissolved in the fuel-water emulsion on the parameters of the CI engine* [in:] *IOP Conference Series: Materials Science and Engineering*, Vol. 148, 2016, pp. 1-8.

[26] Gupta R.K., Sankeerth K.A., Sharma T.K., Rao G., Murthy K.M., *Effects of water-diesel emulsion on the emission characteristics of single cylinder direct injection diesel engine – A review*, Applied Mechanics and Materials, Vol. 592, 2014, pp. 1526-1533.

[27] Kornienko V., Radchenko R., Konovalov D., Andreev A., Pyrysunko M., *Characteristics of the rotary cup atomizer used as afterburning installation in exhaust gas boiler flue* [in:] Ivanov V. et al. (eds.), ADSM III (DSMIE 2020), LNME, Springer, Cham 2020, pp. 302-311.

[28] Kornienko V., Radchenko R., Mikielewicz D., Pyrysunko M., Andreev A., *Improvement of characteristics of water-fuel rotary cup atomizer in a boiler* [in:] Tonkonogyi V. et al. (eds.), AMPII. InterPartner 2020, LNME, Springer, Cham 2021, pp. 664-674.

Andrii CHEILYTKO
Sergii ILIN
Zaporizhzhya National University, Ukraine

DOI: 10.53412/jntes-2020-3.4

RESEARCH OF CYCLONE CHARACTERISTICS FOR DRY CLEANING OF GASES FROM DUST

Abstract: *The development and application of new, more efficient dust collection units that will help reduce emissions and conserve some very valuable resources for production is an important area of research. With the growth of innovation in technological enterprises, the number of harmful emissions into the atmosphere is growing. Thus, the ecological condition of the environment deteriorates. The basic analytical dependences which are necessary for construction of a technique of carrying out experiments and calculations of dust catching for concrete working conditions are developed. Methods of calculating cyclones as vortex devices and research of cyclone operation for air purification from dust were investigated. On the basis of the used basic theoretical positions of heat and mass transfer and thermodynamics at carrying out analytical researches the mathematical model was offered. Calculations of new designs of modern cyclones to obtain their geometric dimensions, resistance and dust capture efficiency were presented. Modern cyclones are designed to more effectively remove dust from the air during various types of work.*

Keywords: *modern cyclone, dust collection, mathematical modelling.*

Introduction

In connection with the UN Development Strategy, one of the four main principles is ecology. In the field of thermal energy, the development and application of new, more efficient dust cleaning units, which will help reduce emissions into the atmosphere and save some very valuable resources for production, is of particular interest. Because with the growth of innovation in technological enterprises, the number of harmful emissions into the atmosphere increases. Thus, the ecological condition of the environment deteriorates.

There are several technologies for cleaning the air from dust. Particular attention is paid to cyclone cleaning. The most reliable results from various experiments can be obtained through experiments conducted on physical models. A separate experiment must be performed for each specific design. More general results are obtained using a mathematical model of hydromechanical processes of cyclones. Creating a mathematical model of the movement of dust particles in a swirling flow will assess the impact of various factors on the efficiency of dust control in cyclones.

To determine the nature of the motion of particles transported by the flow in swirling dust air streams, and their deposition on a solid surface requires the calculation of dynamic equations for turbulent flow and particles used the method of calculating gas-dynamic flows, which combines the properties of Euler and Lagrangian approaches, each is a method of “particles in a cell”. An approximation model of the motion of dust particles in the apparatus was created, with the help of which for each type of aerosol the trajectories of its motion in the apparatus are constructed theoretically, having different design parameters of the dust collector. And thus in the future select the most efficient dust collector for each specific type of technological production.

Another new cyclone installation has a relief surface with detachable zones and an upward-facing truncated cone with 2 times lower aerodynamic drag compared to smooth-walled. The reduction of the hydraulic resistance of the cyclone is facilitated by the presence of detachable zones on the relief surfaces. Simulation of turbulent gas flow in a new type of dust collector shows that the calculations of the cyclone flow pattern agree qualitatively satisfactorily with the experimental data; the decrease in the hydraulic resistance of the cyclone with the internal elements in comparison with the smooth-walled devices is due to the adjustment of the flow: a decrease in the tangential velocity with a simultaneous increase in the axial flow velocity in the cyclone.

Literature review

Industrial enterprises purify the air that is supplied not only to the shops, departments, but also removed from them into the atmosphere to prevent air pollution in the enterprise and the residential areas attached to it [1].

Dedusting devices are divided into dust collectors and filters.

Dust collectors include devices in which dust particles are deposited under the action of gravity and inertial forces with a change in speed and direction of air flow. Such devices are dust chambers, cyclones and other devices operating on the basis of centrifugal forces.

Filters are devices in which dusty air is purified by passing through mesh or porous materials (glass wool, gravel, coke, porous paper, fabric, metal mesh) [2].

Dedusting devices can be not only dry but also wet. When using wet dedusting devices, the efficiency of air purification from dust increases.

To date, both the theoretical basis for capturing dust and gas components and methods for calculating various equipment for these purposes have been developed.

Particular attention was paid to cyclone cleaning. The most reliable results can be obtained through experimental experiments conducted on physical models. But for each specific design you need to conduct a separate experiment. More general results can be obtained using a mathematical model of hydromechanical processes of cyclones. Creating a mathematical model of the movement of dust particles in a swirling flow will assess the impact of various factors on the efficiency of dust control in cyclones [3].

To determine the nature of the motion of particles transported by the flow in swirling dust air streams, and their deposition on a solid surface requires the calculation of dynamic equations for turbulent flow and particles used the method of calculating gas-dynamic flows, which combines the properties of Euler and Lagrangian approaches, each is a method of “particles in a cell”. The nature of the motion of particles is significantly influenced by the conditions of their contact with impact with the surface of the dust collector body, and at sufficiently high speeds the reflection of the particlesaw. Mathematical modeling of the separation process reflects the relationship of the motion of solid particles in the apparatus with its efficiency, it allows to obtain the trajectory of particles in different parts of the apparatus, which calculates its efficiency for each type of dust, and it allows for each type of aerosol theoretically, having different design parameters of dust collectors, choose the most efficient design for each specific type of technological production [4].

Another new cyclone installation has a relief surface with detachable zones and an upward-facing truncated cone with 2 times lower aerodynamic drag compared to smooth-walled. The reduction of the hydraulic resistance of the cyclone is facilitated by the presence of detachable zones on the relief surfaces. Simulation of turbulent gas flow in a new type of dust collector shows that the calculations of the cyclone flow pattern agree qualitatively satisfactorily with the experimental data; the numerical values of the energy of turbulent pulsations for smooth-walled and new types of cyclones agree satisfactorily with experimental data on the efficiency of dust collection of these dust collectors; reduction of hydraulic resistance of a cyclone with internal elements in comparison with smooth-walled devices occurs owing to adjustment of a current.

Dust collectors and filters are used to clean the air from the dust removed by exhaust ventilation [5].

Dust collectors include dust chambers, inertial dust collectors and cyclones. The simplest dust collector for purification of the removed air are dust-depositing chambers which work is based on deposition of dust particles of air at low speed of its movement.

In louvered dust collectors, dust is released from the gas stream under the action of inertial forces when changing the direction of gas flow. With the help of louver plates installed in the flue, the gas flow is divided into two parts.

One stream is 80-90% of the total amount of gas and is largely free of dust, the other is 10-20% and it concentrates the bulk of the dust, which is then captured in a cyclone or other, quite efficient dust collector. The movement of gas through the cyclone is due to the pressure drop on the louver.

Of the inertial devices, cyclones have become the most widespread as more efficient and less expensive dust collectors for the rough cleaning of exhaust gases. This type of dust collector differs significantly from dust chambers both in design and principle of operation.

Cyclones have become widespread and are used to trap chips, sawdust and metal dust. Dusty air is supplied by a fan to the upper part of the outer cylinder of the cyclone.

In a cyclone, the air takes a rotational motion, as a result of which centrifugal force develops, mechanical impurities are thrown to the walls, from where they roll into the lower part of the cyclone, which has the shape of a truncated cone. Purified air through the inner cylinder of the cyclone, the so-called exhaust pipe, comes out. The lower part of the cyclone is periodically cleaned.

In the LIOT cyclone, the separation of dust from the air occurs using centrifugal forces arising in the rotational flow of dusty air descending along a helical line. Dust particles are squeezed to the walls and go down. The purified air exits through the central pipe. Cleaning efficiency up to 85%.

Multicyclones are installed at thermal power plants for pre-treatment in combination with other ash capture methods.

A multicyclone is a combination in one unit of many small cyclones with a diameter of 300-400 mm with a total supply of polluted air and a common hopper for ash that has settled. Up to 65-70% of ash is retained in the multicyclone.

Of interest are wet type dust collectors, which have good efficiency. These include centrifugal scrubbers, washing cyclones, Venturi dust collectors, foam dust collectors and others.

Also worth noting are electrostatic precipitators and ultrasonic dust collectors. The principle of operation of the electrostatic precipitator is based on the fact that dust particles, passing with the air through an electric field, receive charges and, attracting, settle on the electrodes, from which they are then removed mechanically.

Ultrasonic dust collectors use the ability of dust particles under the action of a powerful sound stream to coagulate, i.e. to coagulate in a flake, which is very important for the capture of aerosols from the air [6]. These flakes fall into the hopper. The sound effect is created by a siren. The sirens which are issued can be applied in dust-cleaning installations with a productivity up to 15000 m^3/h.

Problem formulation

The described devices for air purification, shops and departments of industrial enterprises, which are removed to the atmosphere by exhaust ventilation, do not exhaust all types of dust collectors and filters used to prevent air pollution in cities.

Despite the existing variety of cleaning devices, cyclones are now the most common for cleaning gases from dust due to their low cost, simplicity and ease of operation. In this regard, the development of perforated cyclone requires research aimed at increasing the degree of dust capture from gases, which is considered in this paper.

The calculation of cyclones is reduced to obtaining their geometric dimensions, resistance and dust collection efficiency.

Currently, the most common method of calculating cyclones is the method of generalization and use of indicators obtained by testing cyclones in industrial conditions or on stands.

The method of calculating cyclones using experimental data is based on determining the diameter of the cyclone by the formula [7]:

$$D_c = \sqrt{\frac{Q_g}{900 \cdot \pi \cdot W_{\text{con}}}} \tag{1}$$

where:

Q_g – volumetric gas flow through the cyclone, m³/h;

W_{con} – conditional flow rate of gas in the cyclone, m/s.

Cyclone resistance is determined by the following equation [8]:

$$\Delta p = \xi_0 \cdot \frac{W_{\text{con}}^2 \cdot \rho}{2} \tag{2}$$

or

$$\Delta p = \xi_0 \cdot \frac{W_{\text{con}}^2 \cdot \gamma}{2g} \tag{3}$$

The speed of the gas in the inlet of the cyclone is determined by the formula:

$$W_{\text{in}} = \sqrt{\frac{2 \cdot \Delta p}{\xi_{\text{in}} \cdot \rho}} \tag{4}$$

High emissions and low efficiency of cyclones led to significant residual dust in the atmosphere, which required both the development of a new design of cyclones and new theoretical solutions and systems for dedusting of gases. Thus, the generalizing design parameter of cyclones is found in the work and its optimal value is determined, which provides the maximum efficiency of the cyclone, and the analytical dependence characterizing the length of the vortex chamber required to capture the minimum dust particles $d_{\min}$ is obtained.

$$L_{\max} = \frac{9D_c}{\varepsilon^2} \cdot \frac{\mu}{\rho_m} \cdot \frac{\sum f}{\pi \cdot R_0 \cdot R_p \cdot \cos\beta} \cdot \frac{R_c}{R_0} \cdot \frac{1}{W_0} \cdot \frac{\left(\frac{R_p}{R_c}\right)^4 \cdot \frac{1}{\cos\beta}}{\left[1 + \frac{R_p}{R_c} + \left(\frac{R_p}{R_c}\right)^3 + \left(\frac{R_p}{R_c}\right)^4\right] \cdot d_{\min}^2} \tag{5}$$

where:

D_c – inner diameter of the cyclone;

μ – coefficient of dynamic viscosity of the cleaned medium;

ρ_m – actual density of the powder;

$\sum f$ – total area of the pipes of the supply of the cleaned medium in the cyclone;

R_0 – twisting arm (distance from the axis of the supply pipe to the axis of rotation of the cyclone);

R_p – inner radius of the cyclone pipe;

W_0 – speed of the cleaning medium at the outlet of the supply pipe.

In the development of large cyclones, their ability to capture dust can be determined on a model of smaller size, but this requires dependencies, which could be converted from model to nature.

Using the dependence determine the size of the dust, which will be caught by the cyclone at the length L of its chamber:

$$d_{\min} = \frac{3D_c}{\varepsilon} \cdot \sqrt{\frac{\mu}{\rho_m} \cdot \frac{1}{W_0} \cdot \frac{\frac{\sum f}{\pi \cdot R_0 \cdot R_p \cdot \cos\beta} \cdot \frac{R_c}{R_0} \cdot \left(\frac{R_p}{R_c}\right)^4}{\left[1 + \frac{R_p}{R_c} + \left(\frac{R_p}{R_c}\right)^3 + \left(\frac{R_p}{R_c}\right)^4\right] \cdot L \cdot \cos\beta}} \tag{6}$$

The speed of movement of the cleaned environment at the outlet of the supply pipe is determined:

$$W_0 = \sqrt{\frac{2\Delta P}{\xi_{\text{in}} \cdot \rho_g}} \tag{7}$$

where:

ΔP – pressure drop on the cyclone;

ρ_g – density of the medium to be cleaned;

ξ_{in} – coefficient of resistance of the cyclone, which is determined as follows:

$$\xi_{\text{in}} = \left[\frac{\frac{R_0}{R_c} \cdot \cos\beta}{\phi_0 \cdot \frac{R_p}{R_c} \left(1 - \frac{\sum f}{\pi \cdot R_0 \cdot R_p \cdot \cos\beta} \cdot \frac{1}{4\text{tg}\alpha_1} \cdot \frac{1}{\varepsilon}\right) \cdot \cos\alpha_1} \right]^2 \tag{8}$$

We obtain the dependence that determines the relationship between the geometric dimensions of the cyclone and its ability to capture dust particles with a diameter of $d_{\min}$ in the following form:

$$d = \frac{3D_c}{\varepsilon \sqrt[4]{\frac{2\Delta P}{\rho_g}}} \cdot \sqrt{\frac{\mu}{\rho_m} \cdot \frac{\frac{\sum f}{\pi \cdot R_0 \cdot R_p \cdot \cos\beta}}{\phi_0 \left(1 - \frac{\sum f}{\pi \cdot R_0 \cdot R_p \cdot \cos\beta} \cdot \frac{1}{4\text{tg}\alpha_1} \cdot \frac{1}{\varepsilon}\right) \cdot \cos\alpha_1} \cdot \frac{\left(\frac{R_p}{R_c}\right)^4}{\left[1 + \frac{R_{mp}}{R_c} + \left(\frac{R_p}{R_c}\right)^3 + \left(\frac{R_p}{R_c}\right)^4\right] \cdot L}} \tag{9}$$

For geometrically similar cyclones:

$$\frac{d}{D_c} = \frac{C}{\varepsilon} \cdot \sqrt[4]{\frac{\rho_g}{2\Delta P}} \cdot \sqrt{\frac{\mu_g}{\rho_m}} \cdot \sqrt{\frac{1}{L}} \tag{10}$$

where C = const, and

$$C = 3 \cdot \sqrt{\frac{\frac{\sum f}{\pi \cdot R_0 \cdot R_p \cdot \cos\beta}}{\phi_0 \left(1 - \frac{\sum f}{\pi \cdot R_0 \cdot R_p \cdot \cos\beta} \cdot \frac{1}{4\text{tg}\alpha_1} \cdot \frac{1}{\varepsilon}\right) \cdot \cos\alpha_1} \cdot \frac{\left(\frac{R_p}{R_c}\right)^4}{\left[1 + \frac{R_p}{R_c} + \left(\frac{R_p}{R_c}\right)^3 + \left(\frac{R_p}{R_c}\right)^4\right]}} \tag{11}$$

We determine the constant C:

$$C = \frac{d}{D_c} \cdot \varepsilon \cdot \sqrt[4]{\frac{2\Delta P}{\rho_g}} \cdot \sqrt{\frac{\rho_m}{\mu_g}} \cdot \sqrt{L} \tag{12}$$

For two similar cyclones, one of which is denoted by 1, the other – 2, we obtain:

$$\frac{d_1}{D_{c1}} \cdot \varepsilon_1 \cdot \sqrt[4]{\frac{2\Delta P_1}{\rho_{g1}}} \cdot \sqrt{\frac{\rho_{m1}}{\mu_{g1}}} \cdot \sqrt{L_1} = \frac{d_2}{D_{c2}} \cdot \varepsilon_2 \cdot \sqrt[4]{\frac{2\Delta P_2}{\rho_{g2}}} \cdot \sqrt{\frac{\rho_{m2}}{\mu_{g2}}} \cdot \sqrt{L_2} \tag{13}$$

From where the proportion of dust caught in the first cyclone will be determined by the size of the captured dust of the second cyclone according to the following expression:

$$d_1 = d_2 \cdot \frac{D_{c1}}{D_{c2}} \cdot \frac{\varepsilon_2}{\varepsilon_1} \cdot \left(\frac{\Delta P_2}{\Delta P_1}\right)^{0.25} \cdot \left(\frac{\rho_{g1}}{\rho_{g2}}\right)^{0.25} \cdot \left(\frac{\rho_{m2}}{\rho_{m1}}\right)^{0.5} \cdot \left(\frac{\mu_{g1}}{\mu_{g2}}\right)^{0.5} \cdot \left(\frac{L_2}{L_1}\right)^{0.5} \tag{14}$$

since $\mu = \rho \cdot \nu$, then

$$\left(\frac{\rho_{g1}}{\rho_{g2}}\right)^{0.25} \cdot \left(\frac{\rho_{g1}}{\rho_{g2}}\right)^{0.5} \cdot \left(\frac{\nu_1}{\nu_2}\right)^{0.5} = \left(\frac{\rho_{g1}}{\rho_{g2}}\right)^{0.75} \cdot \left(\frac{\nu_{g1}}{\nu_{g2}}\right)^{0.5} \tag{15}$$

then

$$d_1 = d_2 \cdot \frac{D_{c1}}{D_{c2}} \cdot \frac{\varepsilon_2}{\varepsilon_1} \cdot \left(\frac{\Delta P_2}{\Delta P_1}\right)^{0.25} \cdot \left(\frac{\rho_{\varepsilon 1}}{\rho_{\varepsilon 2}}\right)^{0.75} \cdot \left(\frac{\rho_{m2}}{\rho_{m1}}\right)^{0.5} \cdot \left(\frac{\nu_{\varepsilon 1}}{\nu_{\varepsilon 2}}\right)^{0.5} \cdot \left(\frac{L_2}{L_1}\right)^{0.5} \tag{16}$$

or

$$\frac{d_1}{d_2} = \frac{D_{c1}}{D_{c2}} \cdot \frac{\varepsilon_2}{\varepsilon_1} \cdot \left(\frac{\Delta P_2}{\Delta P_1}\right)^{0.25} \cdot \left(\frac{P_{g1}}{P_{g2}}\right)^{0.75} \cdot \left(\frac{T_{g2}}{T_{g2}}\right)^{0.75} \cdot \left(\frac{\mu_1}{\mu_2}\right)^{0.75} \cdot \left(\frac{\rho_{m2}}{\rho_{m1}}\right)^{0.5} \cdot \left(\frac{\rho_{m2}}{\rho_{m1}}\right)^{0.5} \cdot \left(\frac{\nu_{g1}}{\nu_{g2}}\right)^{0.5} \cdot \left(\frac{L_2}{L_1}\right)^{0.5} \tag{17}$$

If under index 2 to denote a model cyclone, and under index 1 – a natural variant, the test results of a model cyclone for dust capture with a diameter of d_2 can be converted into dust capture by a natural cyclone d_1.

Results and Discussions

Thus, if the cyclone model is made reduced by 10 times compared to nature, i.e., $D_{c1} = 10 \cdot D_{c2}$, $L_1 = 10 \cdot L_2$, and the other values of the dependence were the same, in this case $d_2 = d_{2\min}$ = 20 μm, then:

$$d_{1\min} = 20 \cdot \frac{10 \cdot D_2}{D_2} \cdot \left(\frac{L_2}{10 \cdot L_2}\right)^{0.5} = 20 \cdot \frac{10}{3.16} \tag{18}$$

That is, it increases 3 times, which will reduce efficiency.

It is known that as the diameter of the cyclone increases, its efficiency decreases, as evidenced by the experimental data presented in Figure 1.

Gas density $\rho_g = \frac{P_g}{R \cdot T_g}$, then

$$\left(\frac{\rho_{g1}}{\rho_{g2}}\right)^{0.75} = \left(\frac{P_{g1}}{R_1 \cdot T_{g1}} \cdot \frac{R_2 \cdot T_{g2}}{P_{g2}}\right)^{0.75} = \left(\frac{P_{g1}}{P_{g2}}\right)^{0.75} \cdot \left(\frac{T_{g2}}{T_{g1}}\right)^{0.75} \cdot \left(\frac{R_2}{R_1}\right)^{0.75} \tag{19}$$

$$\varepsilon = \frac{M_{0\text{ut}}}{M_{\text{in}}} = \frac{C_1 \cdot \cos\alpha_1 \cdot R_{mp}}{W_0 \cdot R_0} = \frac{C_{ump} \cdot R_{mp}}{W_0 \cdot R_0} = C_1 \cdot \cos\alpha_1 \cdot \frac{R_p}{R_0} \cdot \sqrt{\frac{\xi_{\text{in}} \cdot \rho_{\text{з}}}{2\Delta P}} = \tag{20}$$

$$= \frac{Q}{F_p} \cdot \frac{\cos\alpha_1}{\sin\alpha_1} \cdot \frac{R_{mp}}{R_0} \cdot \frac{\sum f}{Q} = \frac{\sum f}{F_p} \cdot \frac{R_{mp}}{R_0} \cdot \text{ctg}\alpha_1$$

$$\frac{\varepsilon_2}{\varepsilon_1} = \frac{\sum f_2}{\sum f_1} \cdot \frac{F_{p1}}{F_{p2}} \cdot \frac{R_{p2}}{R_{p1}} \cdot \frac{R_{01}}{R_{02}} \cdot \frac{\text{tg}\alpha_2}{\text{tg}\alpha_1} = \frac{\sum f_2}{10\sum f_2} \cdot \frac{10F_{p2}}{F_{p2}} \cdot \frac{10R_{02}}{R_{02}} = 10 \tag{21}$$

$$\frac{\varepsilon_2}{\varepsilon_1} = \frac{\left(\frac{\sum f}{F_p}\right)_2}{\left(\frac{\sum f}{F_p}\right)_1} \cdot \frac{\left(\frac{R_p}{R_0}\right)_2}{\left(\frac{R_p}{R_0}\right)_1} \cdot \frac{(\text{ctg}\alpha_1)_2}{(\text{ctg}\alpha_1)_1} = 1 \tag{22}$$

since they are geometrically similar.

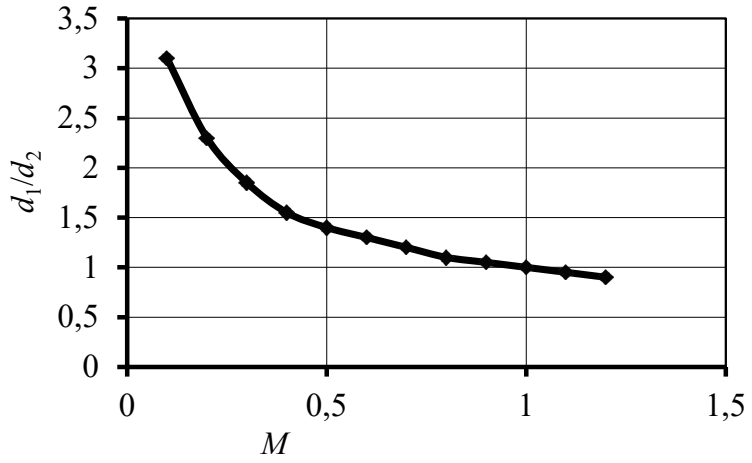

FIGURE 1. *Changing the diameter of the captured dust by a natural cyclone from changing the scale of the model cyclone*

In order for the gas to flow through the dust bypass pipe (flow) from the hopper to the entrance to the dust collector, and not vice versa, it is necessary to calculate the minimum cross-sectional area of the Venturi pipe so that the pressure in this section would be less than the hopper pressure. The movement of gas flows, the values of cross-sectional areas and pressures are showing Figure 2. Experiments have shown that it is the high pressure observed in the upper perforated chamber of the dust collector.

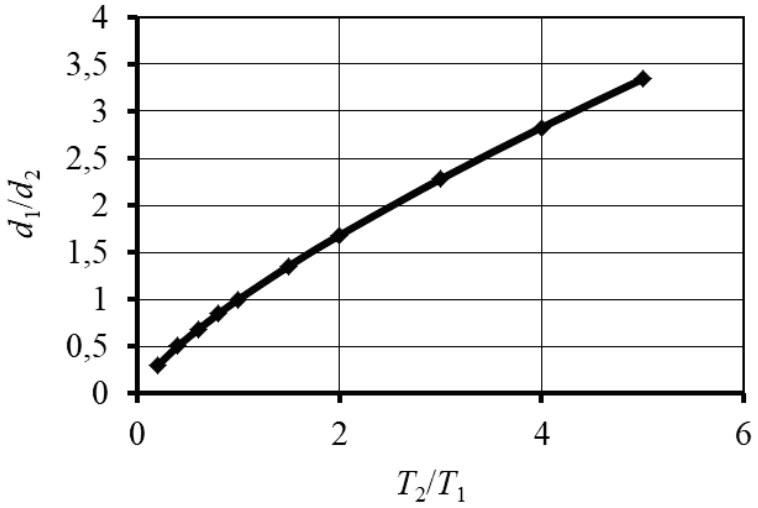

FIGURE 2. *The effect of temperature changes on the diameter of the trapped dust*

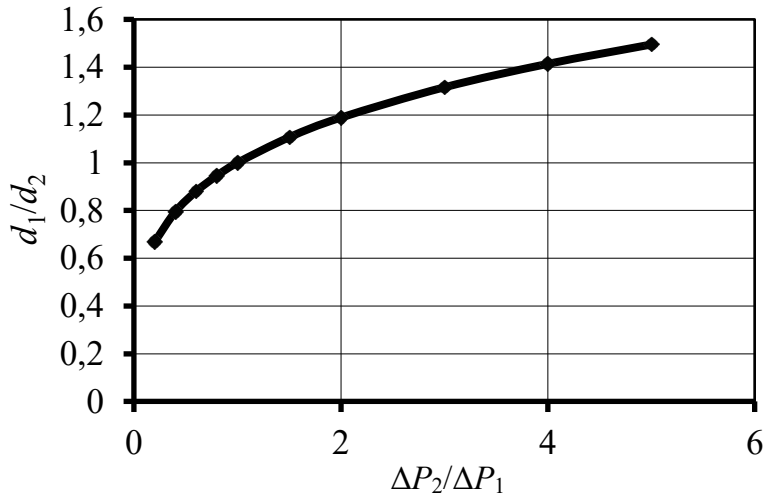

FIGURE 3. *Influence of change of pressure difference on diameter of the caught dust*

Conclusions

Cyclones are widely used in industry. There is a great variety of works devoted to the study of the parameters of cyclones and are private, episodic. The great variety of the offered dependences for calculation of their parameters testifies to complexity of the solved scientific problem which does not have the unambiguous answer yet. Despite the adequacy of aerodynamic processes occurring in cyclones, there is currently no single method for calculating the characteristics of the most common in the industry cyclone-vortex devices. The lack of scientifically sound theoretical developments summarizing the large accumulated material for the study of various cyclones prevents the development of scientific and technological progress in the field of creation and improvement of existing cyclones.

As a result of the theoretical researches carried out in work analytical dependences of the basic parameters of a dust collector are defined. These dependencies make it possible to conduct experimental studies of the dust collector and build a streamlined method of calculating dust collectors of new design, which will allow you to design dust collectors with maximum efficiency for specific operating conditions.

Conflicts of Interest: The author declares no conflict of interest.

REFERENCES

[1] Schaurberger V., *The Energy Evolution: Harnessing Free Energy from Nature*, ed. by Coast C., Gill & Macmillan Ltd., 2000, p. 268.

[2] Taleyarkhan R.P., *Evidence for Nuclear Emissions During Acoustic Cavitation*, Science, 8 March 2002, 295 (5561), pp. 1868-1873, doi:10.1126/science.1067589.

[3] Meyer E. Kuttruff H., *Zur Phasenbeziehung zwischen Sonolumineszenz und Kavitations-vorgang bei periodischer Anregung*, Zeit. Angew. Phys, 1959, 11, pp. 325-333.

[4] Jones S.E., Palmer E.P., Czirr J.B., Decker D.L., Jensen G.L., Thorne J.M., Rafelski J., *Observation of cold nuclear fusion in condensed matter*, Nature, 27 April 1989, 338 (6218), pp. 737-740, doi:10.1038/338737a0.

[5] *The Race for Cold Fusion*, Cold Fusion, Princeton University Press, 1991, pp. 52-69, doi:10.1515/9781400861606.52.

[6] Sorokodum E., *On general nature of forces*, New Energy Technologies, January-February 2002, 1 (4), pp. 30-36. Golubtsov VM Calculation of the twist angle at the outlet of vortex gas burners // Gas industry. 1976. №7. 44c.

[7] Golubtsov V.M., *To calculate the number of vortex blades of vortex burner devices*/*Heat Power Engineering*, pp. 73-75.

[8] Petrakov A.D., Sannikov S.T., Yakovlev O.P., Rotornyi nasos – teplogenerator, patent RF 2159901: MPK 7 F24J3/00, F25B30/00. Appl. No. 98115256/06. Filed 07.08.1998. Bull. No. 12.

[9] Petrakov A.D., Radchenko S.M., Yakovlev O.P., Assignee: Limited Liability Company "Radex", 20.04.2003, Rotornyi gidroudarnyi nasos – teplogenerator, patent RF 2202743: MPK 7 F24J3/00, Appl. No. 2001115428/06, Filed 07.06.2001.

Mykola I. RADCHENKO[1]
Tadeusz BOHDAL[2]
Andrii M. RADCHENKO[1]
Eugeniy I. TRUSHLIAKOV[1]
Volodymyr Y. LABAY[3]
Veniamin S. TKACHENKO[1]

[1] *Admiral Makarov National University of Shipbuilding, 9 Heroes of Ukraine Avenue, Mykolayiv, Ukraine*

[2] *Koszalin University of Technology, 2 Śniadeckich Street, Koszalin 75-453, Poland*

[3] *Lviv Polytechnic National University, 12 Bandera Street, Lviv, Ukraine*

DOI: 10.53412/jntes-2020-3.5

INNOVATIVE AIR CONDITIONING SYSTEM WITH RATIONAL DISTRIBUTION OF THERMAL LOAD

Abstract: *The efficiency of air conditioning (AC) systems depends on the operation of their air coolers at varying heat loads in response to current changeable climatic conditions. The intensity of heat transfer of refrigerant, evaporated inside air coils, drops at the final stage of evaporation, that is caused by drying out the inner wall surface. This results in lowering the overall heat transfer coefficient and reduction of air cooler efficiency in the whole. The concept of overfilling air coils that leads to excluding a dry-out of their inner surface and falling the overall heat transfer intensity at variation of refrigerant flows in response to change of current thermal load on air coolers is developed.*

Keywords: *air conditioning system, heat transfer coefficient.*

Introduction

Air conditioning (AC) systems have grown wide application practically in all fields of human activities: comfort AC in building [1-3] and technological AC in food processing [4-6], gas, oil [7-9] and other technologies, in transport applications, including railway [10-12] and ship [13-15].

They are applied as independent systems as well as subsystems in integrated energy plants (IEP) [16-18] for combined cooling, heat and power (CCHP) or trigeneration [19-21].

The efficiency of AC systems depends on the operation of the whole waste heat recovery complex including extracting the heat into atmosphere by cooling towers [22, 23] and utilizing the exhaust heat from combustion engines [24-26]. Complex waste heat recovery with deep exhaust heat utilization by applying low temperature condensing surfaces [27-29], thermopressor [30-32], ejector [33, 34] and other jet devices [35, 36] and turboexpander technologies [37, 38] are used to enhance the cooling potential and efficiency of AC systems.

The performance efficiency of air conditioning (AC) systems depends on the heat efficiency of their heat exchangers. A lot of publications are devoted to intensification of heat transfer in evaporators [39-41] and condensers [42-44], enhancement of hydrodynamics in minichannel heat exchangers [45, 46] to mitigate flow maldistribution [47, 48], application of two-stage cooling in AC systems for comfort and energetic application [49, 50].

In all cases AC systems operate at variable heat loads in response to actual climatic conditions [50, 51] or have to provide efficient performance of machinery or power plants and combustion engines at

varying climatic conditions. Generally, an overall heat load of any AC system comprises the unstable heat load range, corresponding to ambient (outdoor) air processing with considerable heat load fluctuations in response to actual climatic conditions, and a comparatively stable heat load part for subsequent air cooling (subcooling) to a target temperature [49, 50]. The ambient air precooling mode with considerable heat load fluctuation needs load modulation, whereas the comparatively stable heat load range can be covered by operation of refrigerant compressor at about nominal mode.

In modern variable refrigerant flow (VRF) systems the load modulation is performed by varying refrigerant feed to air coolers [52, 53]. But the problem of inefficient operation of air coolers caused by dry-out of inner walls at the final stage of refrigerant evaporation remains unsolved [49].

The intensity of heat transfer of refrigerant, evaporated inside air coils of air coolers, drops at the final stage of evaporation, that is caused by drying out the inner wall surface while transition of refrigerant two-phase flow from annular to disperse (mist) flow. A sharp decrease in heat transfer coefficient to refrigerant at the final stage of its evaporation in compact air coolers results in lowering the overall heat transfer coefficient and reduction of air cooler efficiency.

A concept of efficient operation of air coolers due to incomplete refrigerant evaporation by injector recirculation of liquid refrigerant that excludes the final burn-out stage of evaporation with drop in intensity of evaporation heat transfer was considered in [49].

A new impulse for further realization of this concept is forced due to applying a circulation of liquid refrigerant, i.e. over filling all the coils of air cooler, that excludes a drop in intensity of evaporation heat transfer leading to overall heat transfer intensity decrease and, as result, the influence of variation in refrigerant flows in response to change of current thermal load on air coolers.

The aim of research is to developed a concept of incomplete refrigerant evaporation with overfilling air coils that leads to excluding a dry-out of their inner surface and falling the overall heat transfer intensity while variation in refrigerant flows in response to change of current thermal loads on air coolers.

Research Methodology

The main idea behind the rational designing and operation of ambient air conditioning systems to match current varying heat loads is sharing the overall heat load in unstable heat load range, corresponding to ambient air processing with considerable load fluctuations in response to actual climatic conditions, and a comparatively stable heat load part for subsequent air cooling (subcooling).

A rational design overall refrigeration capacity $Q_{0.10\text{rat}}$ for cooling ambient air for instance to t_{a2} = 10°C is selected to provide a maximum annular refrigeration energy generation according to AC duties and shared into a comparatively stable basic load and a remaining part for ambient air precooling at varying heat loads [49].

All the calculation results are presented for the refrigeration capacity in relative values of specific refrigeration capacity q_0 as the overall refrigeration capacity Q_0, kW, referred to the unit of air mass flow G_a : $q_0 = Q_0 / G_a$, kW/(kg/s), or kJ/kg; G_a – air mass flow in air cooler, kg/s.

With this the values of specific refrigeration capacity $q_{0.15}$ for cooling ambient air from its current temperature t_{amb} to the temperature t_{a2} = 15°C and $q_{0.10}$ for cooling ambient air to t_{a2} = 10°C and specific refrigeration capacity $q_{0.10–15}$ as their difference $q_{0.10–15} = q_{0.10} - q_{0.15}$ for subcooling air from t_{a2} = 15°C to t_{a2} = 10°C have been calculated for current climatic conditions.

A remaining available part $q_{0.\text{A}10–15}$ for ambient air precooling at varying heat loads is calculated as difference $q_{0.\text{A}10–15} = q_{0.10} - q_{0.10–15}$.

This study takes into account long term annual weather data collected in the weather datasets of various meteorological centres by using “on-line” programs like “mundomanz.com” or others.

Results of investigation

Typical structures of inside tube refrigerant evaporation and behaviour of refrigerant heat transfer coefficients α_a with the vapor mass fraction *x* are presented in Figure 1.

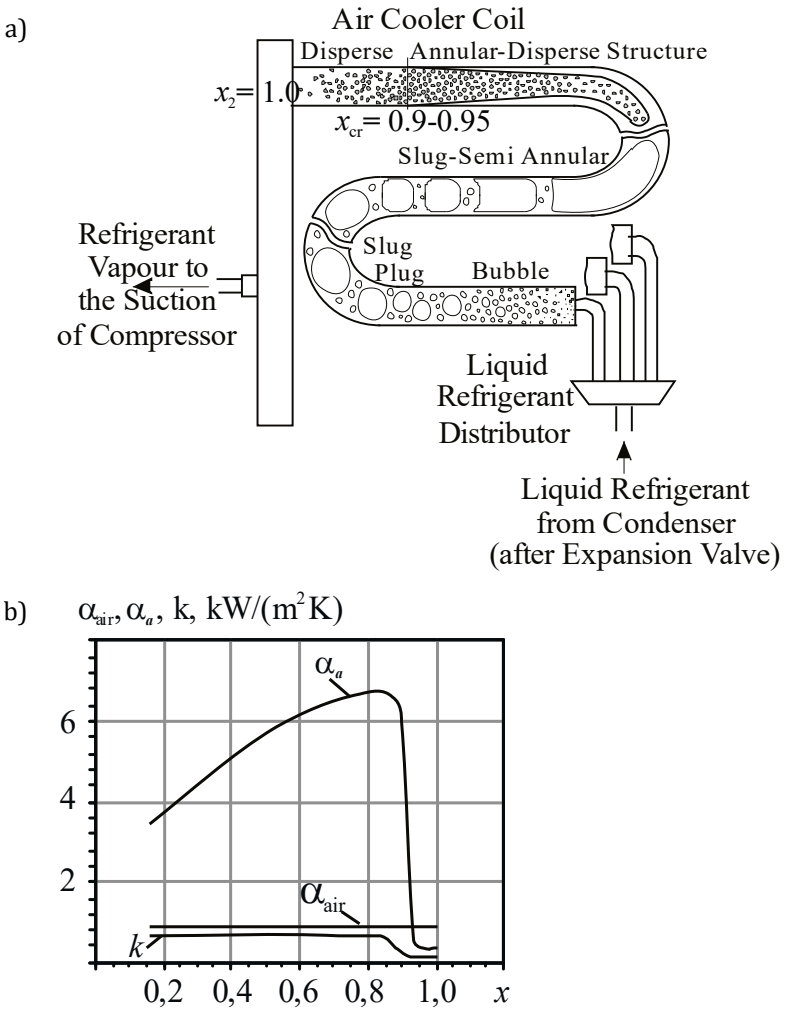

FIGURE 1. *Typical structures of in tube refrigerant boiling (a) and variation of heat transfer coefficients to boiling refrigerant α_a and air α_{air} and overall heat transfer coefficient k with the vapor mass fraction x (b)*

The convective evaporation of refrigerant inside channels is characterized by sharp drop in intensity of heat transfer at the final stage of evaporation when so called burnout takes place. This occurs due to inner channel wall surface drying out with transition of refrigerant two-phase flow from annular-disperse flow to disperse (mist) flow (Fig. 1a).

In compact air coolers with finned tubes the coefficient of heat transfer to refrigerant α_a at the final stage of its evaporation is much lower than α_{air} to air. This results in decrease in overall heat transfer coefficient *k* (Fig. 1b).

Calculations are performed for the air cooler with plate finned tubes of 12 mm and 10 mm outside and inside diameters, air temperature at the inlet t_{air1} = 25°C and outlet t_{air2} = 15°C, refrigerant boiling temperature at the exit t_{02} = 0°C, refrigerant R142b.

Considerable lowering the heat transfer coefficient to refrigerant α_a which becomes lower than the heat transfer coefficient to air α_{air} and causes a decrease in the overall heat transfer coefficient *k* at burnout vapor fraction $x_{cr} \approx 0.9$ corresponding to drying the channel wall surface with the transition from annular to disperse flow that leads to the sharp decrease in the heat flux *q*.

To provide intensive heat transfer on all the length of air cooler coils it is necessary to exclude their ending post dry out sections, i.e. make the air coolers operate with incomplete boiling. The unevaporated liquid should be separated from the vapour in the liquid separator and directed again at the entrance of air cooler.

The results of thermal efficiency comparison of conventional air cooler with complete evaporation and superheated vapor at the exit and of advanced air cooler with incomplete evaporation are shown in Figure 2.

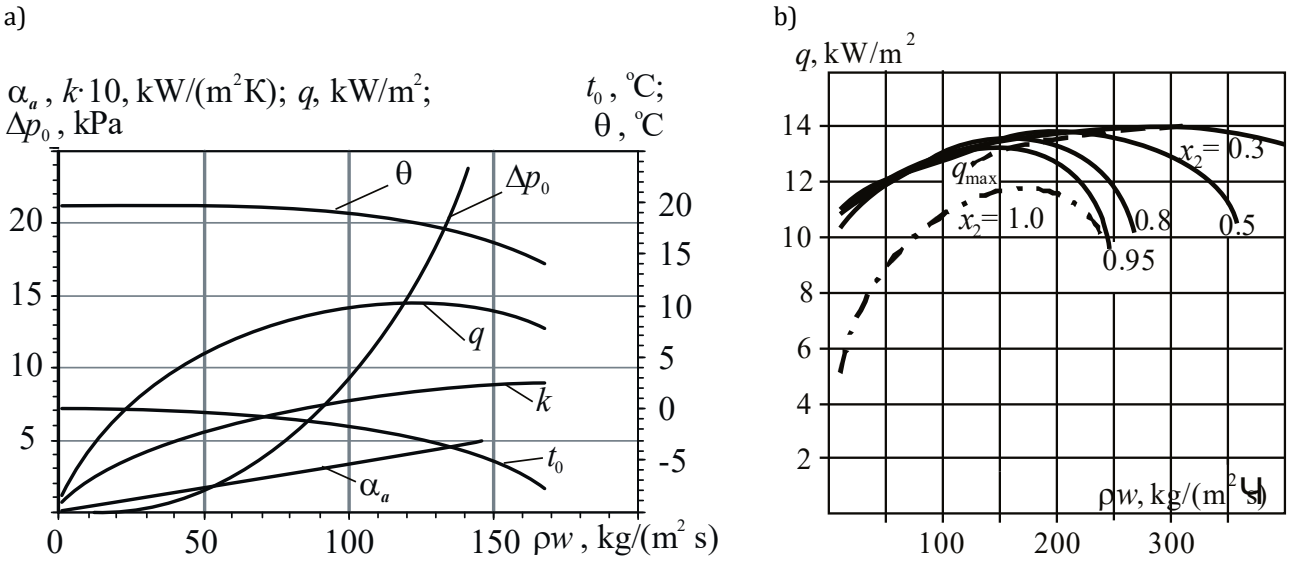

Figure 2. *Mean values of heat fluxes q, heat transfer coefficients to refrigerant α_a and overall heat transfer coefficients k, logarithmic temperature difference θ, refrigerant boiling temperature t_0 and pressure drop ΔP against refrigerant mass velocities ρw for complete evaporation (a) and heat fluxes q at mass vapor fraction x_2 at the outlet of air coil for incomplete refrigerant evaporation (b): R142b, t_{02} = 0°C; air velocity w = 6 m/s*

Thus, overfilling the air coils of the air cooler by liquid refrigerant provides an increase in heat flux q by 25%, …, 40% compared with conventional complete refrigerant evaporation and enables a larger deviation of refrigerant mass velocities ρw from their optimum value, providing maximum value of heat flux q. This means that larger heat load changes are permitted, that give good perspectives for application of overfilling the air coolers by liquid refrigerant in ambient air conditioning systems characterized by considerable fluctuations of loading.

To prove a methodological approach to determine a design heat load, matching current changeable climatic conditions, the values of specific refrigeration capacity $q_{0.15}$ for cooling ambient air from its current temperature t_{amb} to the temperature t_{a2} = 15°C and $q_{0.10}$ for cooling ambient air from t_{amb} to t_{a2} = 10°C and specific refrigeration capacity $q_{0.10–15}$ as their difference $q_{0.10–15} = q_{0.10} - q_{0.15}$ for cooling air from t_{a2} = 15°C to t_{a2} = 10°C have been calculated for climatic conditions in Nikolaev region, southern Ukraine, in July 2015 (Fig. 3).

As can be seen from Figure 3, with cooling the ambient air from t_{amb} to t_{a2} = 15°C the fluctuations in the current heat load $q_{0.15}$ on the air cooler of AC system are very significant. But when air is being cooled from t_{a2} = 15°C to t_{a2} = 10°C, the fluctuations of the heat load on the air cooler of AC system $q_{0.10–15} = q_{0.10} - q_{0.15}$ are relatively small: from 10 kW/(kg/s) to 12 kW/(kg/s).

Obviously, the range of refrigeration capacity controlling according to heat load can be narrowed by dividing the current heat load range on the air cooler in two parts: the relatively stable basic part $q_{0.10–15} = q_{0.10} - q_{0.15}$ while cooling air from t_{a2} = 15°C to t_{a2} = 10°C, and its extremely unstable part $q_{0.15}$ of precooling the ambient air from its current temperature t_{amb} to t_{a2} = 15°C.

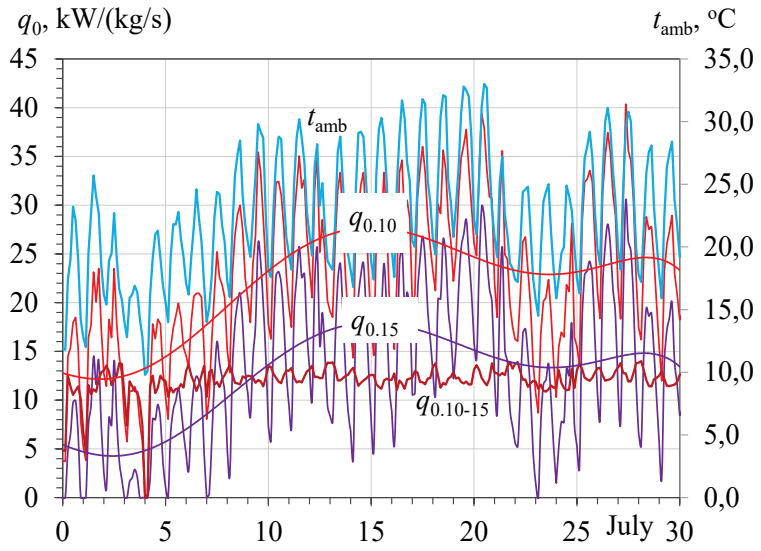

FIGURE 3. *Current values of specific refrigeration capacity $q_{0.15}$ for cooling ambient air from t_{amb} to t_{a2} = 15°C, $q_{0.10}$ for cooling ambient air from t_{amb} to t_{a2} = 10°C and refrigeration capacity $q_{0.10\text{-}15}$ for cooling air from t_{a2} = 15°C to t_{a2} = 10°C: $q_{0.10\text{-}15} = q_{0.10} - q_{0.15}$*

So, the stable heat load value $q_{0.10–15}$ is chosen as design basic part $q_{0.10–15} = q_{0.10} - q_{0.15}$ of the rational design total heat load $q_{0.10rat}$ about 34 kW/(kg/s), ..., 35 kW/(kg/s) on the whole air cooler of AC system determined according to maximum annual refrigeration energy generation [49].

The available rest part of the total heat load $q_{0.10rat}$ on the whole air cooler might be used for precooling the air from the current changeable ambient temperature t_{amb} to t_{a2} = 15°C and be determined according to a remained principle as available loads $q_{0.A10–15} = q_{0.10rat} - q_{0.10–15}$.

So, the total unstable current heat load $q_{0.10}$ for cooling ambient air from the changeable current ambient temperature t_{amb} to t_{a2} = 10°C can be covered by two stage ambient air cooling (Fig. 4).

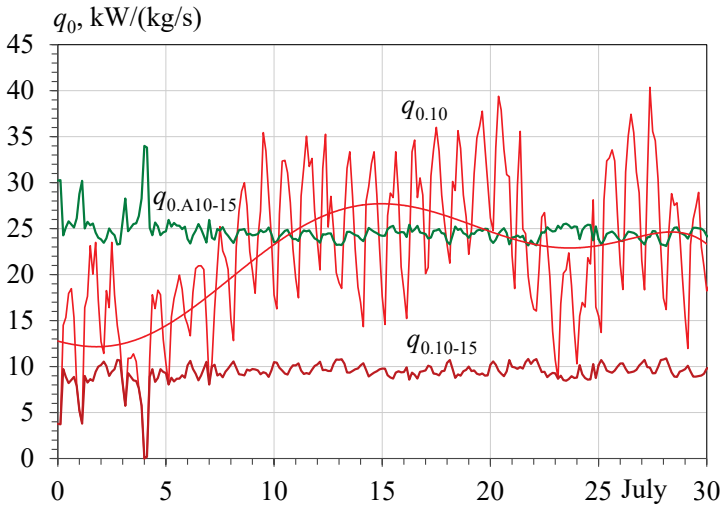

FIGURE 4. *Current values of changeable heat load $q_{0.10}$ for cooling ambient air from t_{amb} to t_{a2} = 10°C covered by available rest specific refrigeration capacity $q_{0.A10\text{-}15}$ and by basic specific refrigeration capacity $q_{0.10\text{-}15}$ for cooling air from t_{a2} = 15°C to t_{a2} = 10°C: $q_{0.10\text{-}15} = q_{0.10} - q_{0.15}$; $q_{0.A10\text{-}15} = q_{0.10rat} - q_{0.10\text{-}15}$*

As Figure 5 shows, the available rest specific refrigeration capacity $q_{0.A10–15}$ generally covers current heat loads $q_{0.15}$ for precooling the air from the ambient temperature t_{amb} to the temperature t_{a2} = 15°C, except a few the warmest quite short periods of daylight hours.

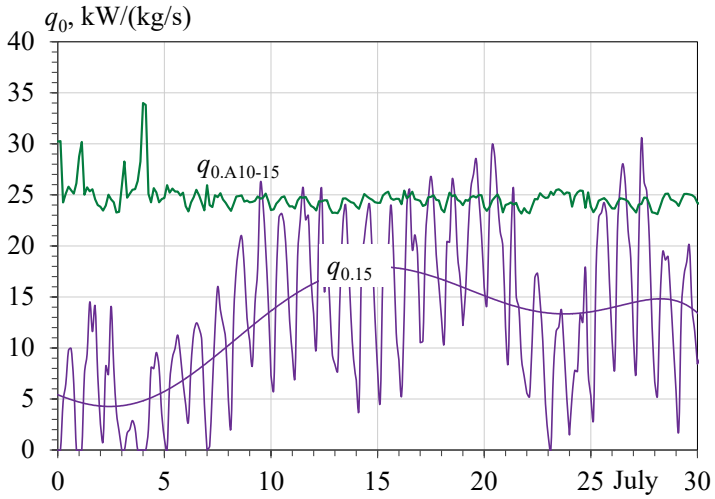

FIGURE 5. *Current values of changeable current heat load $q_{0.15}$ for cooling ambient air from current temperature t_{amb} to t_{a2} = 15°C covered by available rest specific refrigeration capacity $q_{0.A10-15}$*

It is quite reasonable to suppose that the less available rest range of refrigeration capacity for precooling of the ambient air with fluctuations of the current heat load on the air cooler, the lower energy losses caused by the operation of the compressor refrigeration machine in partial modes. But such supposal about more narrow available rest range of refrigeration capacity will be correct if the basic range of refrigeration capacity for futher deep cooling of air from a higher temperature, for example t_{a2} = 20°C, remains stable.

In order to make any conclusion the values of specific refrigeration capacity $q_{0.10}$ for cooling ambient air from its current temperatures t_{amb} to t_{a2} = 10°C are shared in two ranges: refrigeration capacities $q_{0.A10–20} = q_{0.rat} - q_{0.10–20}$ for precooling ambient air from t_{amb} to t_{a2} = 20°C and $q_{0.10–20} = q_{0.10} - q_{0.20}$ for further cooling air from t_{a2} = 20°C to t_{a2} = 10°C have been calculated (Fig. 6).

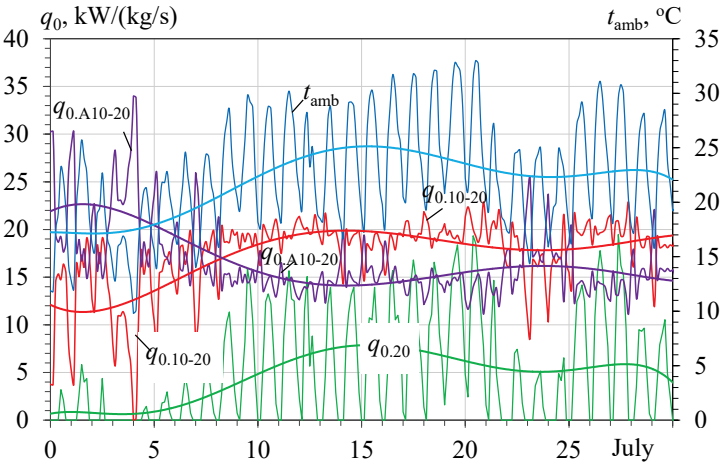

FIGURE 6. *Current values of specific refrigeration capacity $q_{0.20}$ needed for cooling ambient air from t_{amb} to t_{a2} = 20°C, refrigeration capacities $q_{0.A10-20}$ for cooling ambient air from t_{amb} to t_{a2} = 20° and $q_{0.10-20} = q_{0.10} - q_{0.20}$ for further cooling air from t_{a2} = 20°C to t_{a2} = 10°C: $q_{0.10-20} = q_{0.10} - q_{0.20}$; $q_{0.A10-20} = q_{0.rat} - q_{0.10-20}$*

As Figure 6 shows, with precooling the ambient air from t_{amb} to the temperature t_{a2} = 20°C the fluctuations in the current heat loads $q_{0.20}$ on the air cooler of the AC system are very significant. This is caused by daily ambient air temperate t_{amb} dropping lower 20°C (within 1-9 July) with corresponding falling down to zero of the refrigeration capacity $q_{0.20}$ needed. In its turn, this causes decreasing the

refrigeration capacity $q_{0.10–20}$ required for further cooling air from t_{a2} = 20°C to t_{a2} = 10°C and leads to excess of the available rest refrigeration capacity $q_{0.A10–20}$ as compared with $q_{0.20}$ needed.

The excess of available design refrigeration capacities $q_{0.A10–20} = q_{0.10rat} - q_{0.10–20}$ can be used for deeper cooling ambient air, for instance to t_{a2} = 15°C, i.e. to cover heat load $q_{0.15}$ compared with designed $q_{0.20}$ (Fig. 7).

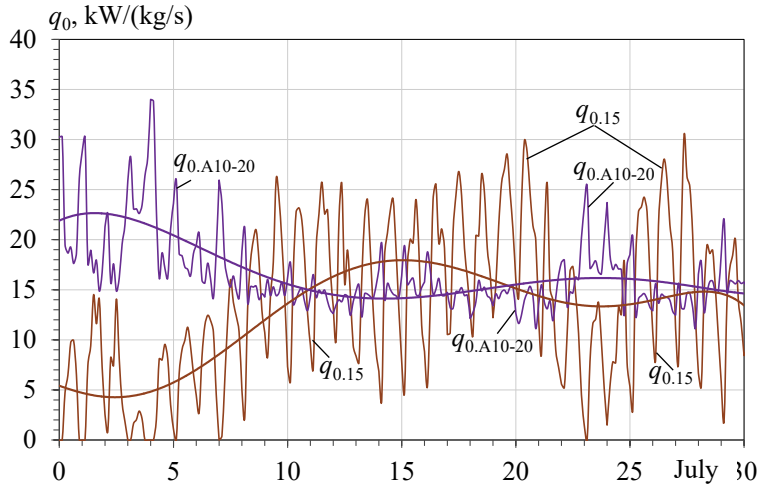

FIGURE 7. *Current values of specific refrigeration capacity $q_{0.15}$ needed for cooling ambient air from t_{amb} to t_{a2} = 15°C and available design refrigeration capacities $q_{0.A10-20} = q_{0.rat} - q_{0.10-20}$*

As it is seen, the available design refrigeration capacities $q_{0.A10–20}$ are considerably higher than refrigeration capacity $q_{0.15}$ needed for cooling ambient air to t_{a2} = 15°C within 1-9 and 22-25 July and lower along the rest daylight time. But large fluctuations of current heat loads $q_{0.15}$ reveal the possibilities to cover a deficit of available design refrigeration capacities $q_{0.A10–20}$ during daylight hours by its excess accumulated within night hours. This leads to reduction of installed refrigeration capacities by the values of $\Delta q_{0.15–20} = q_{0.15} - q_{0.20}$ with using as basic the reduced design refrigeration capacity $q_{0.10–15} = q_{0.10} - q_{0.15}$ instead of $q_{0.10–20} = q_{0.10} - q_{0.20}$ (Fig. 8).

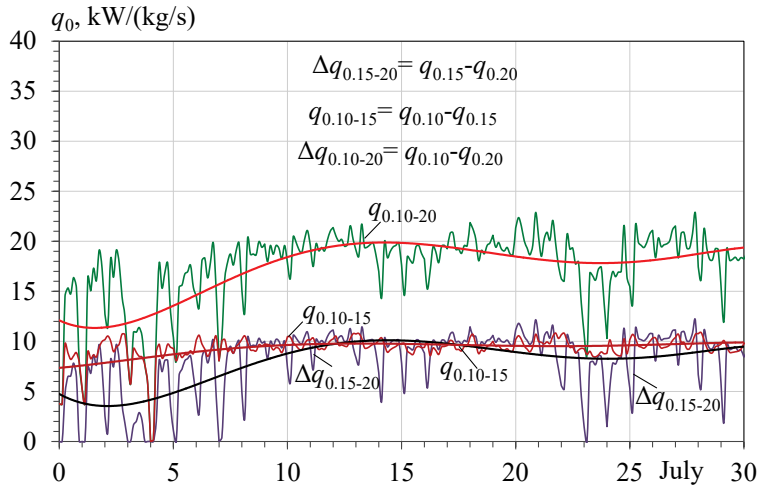

FIGURE 8. *Current values of basic comparatively stable specific refrigeration capacity $q_{0.10-15}$ for cooling air from 15°C to 10°C and $q_{0.10-20}$ for cooling air from 20°C to 10°C and decrease $\Delta q_{0.15-20}$ in design refrigeration capacity: $q_{0.10-15} = q_{0.10} - q_{0.15}$; $q_{0.10-20} = q_{0.10} - q_{0.20}$; $\Delta q_{0.15-20} = q_{0.15} - q_{0.20}$*

The same effect can be realized by decreasing the installed refrigeration capacities for ambient air precooling to t_{a2} = 15°C instead of t_{a2} = 20°C by the same values of $\Delta q_{0.15-20} = q_{0.15} - q_{0.20}$ with using the reduced design refrigeration capacity $q_{0.A10-20} = q_{0.10rat} - q_{0.10-20}$ instead of $q_{0.A10-15} = q_{0.10rat} - q_{0.10-15}$ (Fig. 9).

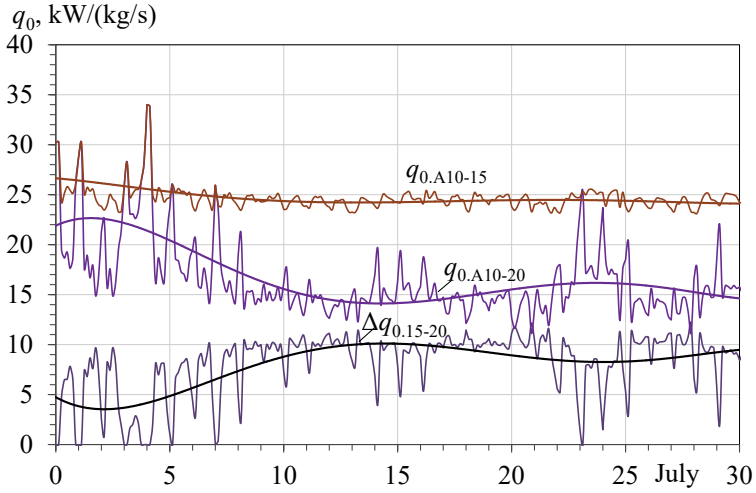

FIGURE 9. *Current values of available remained specific refrigeration capacity $q_{0.A10-20}$ for cooling ambient air 20°C and $q_{0A.10-15}$ for cooling ambient air from t_{amb} to t_{a2} = 15°C and decrease $\Delta q_{0.15-20}$ in design refrigeration capacity: $q_{0.10-15} = q_{0.10} - q_{0.15}$; $q_{0.10-20} = q_{0.10} - q_{0.20}$; $q_{0A.10-15} = q_{0.10rat} - q_{0.10-15}$; $q_{0.A10-20} = q_{0.10rat} - q_{0.10-20}$, $\Delta q_{0.15-20} = q_{0.15} - q_{0.20}$*

It is seen, that a decrease $\Delta q_{0.15-20} = q_{0.15} - q_{0.20}$ in design refrigeration capacity due to its rational distribution with cooling air from t_{a2} = 20°C to t_{a2} = 15°C through using excessive refrigeration capacity of the available remained design value $q_{0.A10-20} = q_{0.10rat} - q_{0.10-20}$ to cover current loads $q_{0.A10-15} = q_{0.10rat} - q_{0.10-15}$ for cooling ambient air to t_{a2} = 15°C instead of t_{a2} = 20°C is about $\Delta q_{0.15-20}$ = 10 kW/(kg/s), that is about 40% of decreased design value $q_{0.10rat} - \Delta q_{0.15-20} \approx$ 25 kW/(kg/s).

As Figure 2b shows, overfilling the air coils of the air cooler by liquid refrigerant allows the variation of refrigerant flows in response to change of current thermal loads on air coolers without considerable drop in heat flux enlarged by about 30% to 50%.

Thus the realization of a concept of incomplete refrigerant evaporation with overfilling air coils enables a larger deviation of refrigerant flows in ambient air coolers of AC system according to current heat load variation without noticeable decrease of heat flux.

Conclusions

A developed concept is intended to enhance the heat efficiency of air coolers at varying heat loads by over filling all the air coils that provides excluding the inner wall surface drying out at the final stage of refrigerant evaporation with low intensity of heat transfer that takes place while complete refrigerant evaporation in conventional air coolers of AC systems.

The overfilling of air coils allows enlarged variation of refrigerant flows in response to change of current thermal loads on air coolers without noticeable drop in heat flux.

The realization of concept of overfilling air coils permits enlarged variation of refrigerant flows in response to change of current thermal loads on air coolers without noticeable drop in heat flux and enables to cover current overloading the air coolers of AC system through increasing refrigerant flows and using the excessive refrigeration energy accumulated at lowered thermal loads.

The effect gained due to overfilling air coolers consists in reduction of installed (design) refrigeration capacity by about 15% to 20% due to covering the currant cooling capacities needed for cooling ambient air to 15°C by installed cooling capacity designed for cooling air to 20°C.

The main idea behind the principle of rational designing and operation of ambient AC systems to match current varying heat loads is sharing the overall heat load in unstable heat load range, corresponding to ambient air processing with considerable heat load fluctuations in response to actual climatic conditions, and a comparatively stable heat load part for subsequent air cooling to a target temperature.

The overfilling all the air coils by liquid refrigerant enables to match actual changeable heat loads not by varying compressor refrigerant capacity but through supplying the excessive refrigerant accumulated at lowered thermal loads on air coolers.

The air coolers based on the principle of overfilling can find a wide application in ambient air conditioning with great fluctuations of current heat loads to cover a deficit of installed (design) refrigeration capacity at arised current heat loads through using its excess at lowered loads and thereby reduce installed (design) refrigeration capacity by about 20%.

REFERENCES

[1] Rodriguez-Aumente P.A., Rodriguez-Hidalgo M.C., Nogueira J.I., Lecuona A., Venegas M.C., *District heating and cooling for business buildings in Madrid*, Applied Thermal Engineering, Vol. 50, 2013, pp. 1496-1503.

[2] Ortiga J., Bruno J.C., Coronas A., *Operational optimization of a complex trigeneration system connected to a district heating and cooling network*, Applied Thermal Engineering, Vol. 50, 2013, pp. 1536-1542.

[3] Trushliakov E., Radchenko A., Radchenko M., Kantor S., Zielikov O., *The Efficiency of refrigeration capacity regulation in the ambient air conditioning systems* [in:] Ivanov V. et al. (eds.), *Advances in Design*, Simulation and Manufacturing III (DSMIE 2020), LNME, Springer, Cham 2020, pp. 343-353.

[4] Freschi F., Giaccone L., Lazzeroni P., Repetto M., *Economic and environmental analysis of a trigeneration system for food-industry: A case study*, Appl. Energy, Vol. 107, 2013, pp. 157-172, doi:10.1016/j.apenergy.2013.02.037.

[5] Trushliakov E., Radchenko A., Forduy S., Zubarev A., Hrych A., *Increasing the Operation Efficiency of Air Conditioning System for Integrated Power Plant on the Base of Its Monitoring* [in:] Nechyporuk M., Pavlikov V., Kritskiy D. (eds.), ICTME (ICTM 2019), AISC, Springer, Vol. 1113, Cham 2020, pp. 351-360, https://doi.org/10.1007/978-3-030-37618-5_30.

[6] Radchenko A., Scurtu I-C., Radchenko M., Forduy S., Zubarev A., *Monitoring the efficiency of cooling air at the inlet of gas engine in integrated energy system*, Thermal Science, 2020, OnLine-First Issue 00, pp. 344-344, https://doi.org/10.2298/TSCI200711344R.

[7] Popli S., Rodgers P., Eveloy V., *Trigeneration scheme for energy efficiency enhancement in a natural gas processing plant through turbine exhaust gas waste heat utilization*, Appl. Energy, Vol. 93, 2012, pp. 624-636, doi:10.1016/j.apenergy.2011.11.038.

[8] Popli S., Rodgers P., Eveloy V., *Gas turbine efficiency enhancement using waste heat powered absorption chillers in the oil and gas industry*, Applied Thermal Engineering, Vol. 50, 2013, pp. 918-931, doi:10.1016/j.applthermaleng.2012.06.018.

[9] Radchenko A., Radchenko N., Tsoy A., Portnoi B., Kantor S., *Increasing the efficiency of gas turbine inlet air cooling in actual climatic conditions of Kazakhstan and Ukraine*, AIP Conference Proceedings, Vol. 2285, 2020, No. 030071, https://doi.org/10.1063/5.0026787.

[10] Radchenko M., Radchenko R., Tkachenko V., Kantor S., Smolyanoy E., *Increasing the Operation Efficiency of Railway Air Conditioning System on the Base of Its Simulation Along the Route Line* [in:] Nechyporuk M. et al. (eds.), ICTME (ICTM 2019), AISC, Springer, Vol. 1113, Cham 2020, pp. 461-467, https://doi.org/10.1007/978-3-030-37618-5_39.

[11] Radchenko N., Radchenko A., Tsoy A., Mikielewicz D., Kantor S., Tkachenko V., *Improving the efficiency of railway conditioners in actual climatic conditions of operation*, AIP Conference Proceedings, Vol. 2285, 2020, No. 030072, https://doi.org/10.1063/5.0026789.

[12] Radchenko M., Mikielewicz D., Tkachenko V., Klugmann M., Andreev A., *Enhancement of the operation efficiency of the transport air conditioning system* [in:] Ivanov V. et al. (eds.), ADSM III (DSMIE 2020), LNME, Springer, Cham 2020, pp. 332-342.

[13] Radchenko R., Pyrysunko M., Radchenko A., Andreev A., Kornienko V., *Ship engine intake air cooling by ejector chiller using recirculation gas heat* [in:] Tonkonogyi V. et al. (eds.), AMP, InterPartner-2020, LNME, Springer, Cham 2021, pp. 734-743.

[14] Radchenko R., Kornienko V., Pyrysunko M., Bogdanov M., Andreev A., *Enhancing the Efficiency of marine diesel engine by deep waste heat recovery on the base of its simulation along the route line* [in:] Nechyporuk M. et al. (eds.), ICTME, AISC, Springer, Vol. 1113, Cham 2020, pp. 337-350.

[15] Radchenko M., Radchenko R., Kornienko V., Pyrysunko M., *Semi-empirical correlations of pollution processes on the condensation surfaces of exhaust gas boilers with water-fuel emulsion Combustion* [in:] Ivanov V. et al. (eds.), DSMIE 2019, LNME, Springer, Cham 2020, pp. 853-862.

[16] Forduy S., Radchenko A., Kuczynski W., Zubarev A., Konovalov D., *Enhancing the fuel efficiency of gas engines in integrated energy system by chilling cyclic air* [in:] Tonkonogyi V. et al. (eds.), Grabchenko's ICAMP, InterPartner-2019, LNME, Springer, Cham 2020, pp. 500-509, https://doi.org/10.1007/978-3-030-40724-7_51.

[17] Radchenko A., Mikielewicz D., Forduy S., Radchenko M., Zubarev A., *Monitoring the fuel efficiency of gas engine in integrated energy system* [in:] Nechyporuk M. et al. (eds.), ICTM 2019, AISC (2020), Springer, Vol. 1113, Cham 2020, pp. 361-370, https://doi.org/10.1007/978-3-030-37618-5_31.

[18] Elberry M., Elsayed A., Teamah M., Abdel-Rahman A., Elsafty A., *Performance improvement of power plants using absorption cooling system*, Alex. Eng. J., Vol. 57, 2018, pp. 2679-2686, doi:10.1016/j.aej.2017.10.004.

[19] Suamir I., Tassou S., *Performance evaluation of integrated trigeneration and CO_2 refrigeration systems*, Appl. Therm. Eng., Vol. 50, 2013, pp. 1487-1495, doi:10.1016/j.applthermaleng.2011.11.055.

[20] Al-Ibrahim A.M., Varnham A., *A review of inlet air-cooling technologies for enhancing the performance of combustion turbines in Saudi Arabia*, Appl. Therm. Eng., Vol. 30, 2010, pp. 1879-1888, doi:10.1016/j.applthermaleng.2010.04.025.

[21] Trushliakov E., Radchenko M., Portnoi B., Tkachenko V., Hrych A., *Analysis of operation of ambient air conditioning systems with refrigeration machines of different types* [in:] Nechyporuk M., Pavlikov V., Kritskiy D. (eds.), ICTME – 2020, ICTM 2020, Lecture Notes in Networks and Systems, Springer, Vol. 188, Cham 2021, pp. 545-555.

[22] Radchenko A., Stachel A., Forduy S., Portnoi B., Rizun O., *Analysis of the Efficiency of Engine Inlet Air Chilling Unit with Cooling Towers* [in:] Ivanov V., et al. (eds.), *Advances in Design, Simulation and Manufacturing III (DSMIE 2020)*, Lecture Notes in Mechanical Engineering, Springer, Cham 2020, pp. 322-331.

[23] Radchenko M., Portnoi B., Kantor S., Forduy S., Konovalov D., *Rational thermal loading the engine inlet air chilling complex with cooling towers* [in:] Tonkonogyi V. et al. (eds.), *Advanced Manufacturing Processes II*, InterPartner 2020, Lecture Notes in Mechanical Engineering, Springer, Cham 2021, pp. 724-733.

[24] Kornienko V., Radchenko M., Radchenko R., Konovalov D., Andreev A., Pyrysunko M., *Improving the efficiency of heat recovery circuits of cogeneration plants with combustion of water-fuel emulsions*, Thermal Science, Vol. 25, Issue 1, Part B, 2021, pp. 791-800, doi: 10.2298/TSCI200116154K.

[25] Kornienko V., Radchenko R., Konovalov D., Andreev A., Pyrysunko M., *Characteristics of the rotary cup atomizer used as afterburning installation in exhaust gas boiler Flue* [in:] Ivanov V. et al. (eds.), ADSM III (DSMIE 2020), LNME, Springer, Cham 2020, pp. 302-311.

[26] Kornienko V., Radchenko R., Mikielewicz D., Pyrysunko M., Andreev A., *Improvement of characteristics of water-fuel rotary cup atomizer in a boiler* [in:] Tonkonogyi V. et al. (eds.), AMPII, InterPartner-2020, LNME, Springer, Cham 2021, pp. 664-674.

[27] Kornienko V., Radchenko R., Stachel A., Andreev A., Pyrysunko M., *Correlations for pollution on condensing surfaces of exhaust gas boilers with water-fuel emulsion combustion* [in:] Tonkonogyi V. et al. (eds.), AMP, InterPartner-2019, LNME, Springer, Cham 2020, pp. 530-539.

[28] Kornienko V., Radchenko R., Bohdal Ł., Kukiełka L., Legutko S., *Investigation of condensing heating surfaces with reduced corrosion of boilers with water-fuel emulsion combustion* [in:] Nechyporuk M. et al. (eds.), ICTM 2020, LNNS, Springer, Vol. 188, Cham 2021, pp. 300-309.

[29] Kornienko V., Radchenko M., Radchenko R., Bohdal Ł., Andreev A., *Thermal characteristics of the wet pollution layer on condensing heating surfaces of exhaust gas boilers* [in:] Ivanov V., et al. (eds.), ADSM IV (DSMIE 2021), LNME, Springer, Cham 2021, pp. 339-348.

[30] Konovalov D., Trushliakov E., Radchenko M., Kobalava G., Maksymov V., *Research of the aerothermopresor cooling system of charge air of a marine internal combustion engine under variable climatic conditions of operation* [in:] Tonkonogyi V. et al. (eds.), ICAMP, InterPartner-2019, LNME, Springer, Cham 2020, pp. 520-529.

[31] Konovalov D., Kobalava H., Radchenko M., Scurtu I.C., Radchenko R., *Determination of hydraulic resistance of the aerothermopressor for gas turbine cyclic air cooling* [in:] TE-RE-RD 2020, E3S Web of Conferences, Vol. 180, No. 0101231, 2020.

[32] Kobalava H., Konovalov D., Radchenko R., Forduy S., Maksymov V., *Numerical simulation of an aerothermopressor with incomplete evaporation for intercooling of the gas turbine engine* [in:] Nechyporuk M., Pavlikov V., Kritskiy D. (eds.), *Integrated Computer Technologies in Mechanical Engineering – 2020*, ICTM 2020, Lecture Notes in Networks and Systems, Springer, Vol. 188, Cham 2021, pp. 519-530.

[33] Butrymowicz D., Gagan J., Śmierciew K., Łukaszuk M., Dudar A., Pawluczuk A., Łapiński A., Kuryłowicz A., *Investigations of prototype ejection refrigeration system driven by low grade heat*, HTRSE-2018, E3S Web of Conferences 70, 2018, p. 7.

[34] Smierciew K., Gagan J., Butrymowicz D., Karwacki J., *Experimental investigations of solar driven ejector air-conditioning system*, Energy and Buildings, Vol. 80, 2014, pp. 260-267.

[35] Trushliakov E., Radchenko M., Bohdal T., Radchenko R., Kantor S., *An innovative air conditioning system for changeable heat loads* [in:] Tonkonogyi V. et al. (eds.), ICAMP, InterPartner-2019, LNME, Springer, Cham 2020, pp. 616-625.

[36] Radchenko N.I., *On reducing the size of liquid separators for injector circulation plate freezers*, International Journal of Refrigeration, Vol. 8, No. 5, 1985, pp. 267-269.

[37] Radchenko A., Andreev A., Konovalov D., Zhang Qiang Z., Zewei L., *Analysis of ship main engine intake air cooling by ejector and turbocompressor chillers on equatorial voyages* [in:] Nechyporuk M., Pavlikov V., Kritskiy D. (eds.), *Integrated Computer Technologies in Mechanical Engineering – 2020*, ICTM 2020, Lecture Notes in Networks and Systems, Springer, Vol. 188, Cham 2021, pp. 487-497.

[38] Radchenko M., Mikielewicz D., Andreev A., Vanyeyev S., Savenkov O., *Efficient ship engine cyclic air cooling by turboexpander chiller for tropical climatic conditions* [in:] Nechyporuk M., Pavlikov V., Kritskiy D. (eds.), *Integrated Computer Technologies in Mechanical Engineering – 2020*, ICTM 2020, Lecture Notes in Networks and Systems, Springer, Vol. 188, Cham 2021, pp. 498-507.

[39] Bohdal T., Kuczynski W., *Boiling of R404A refrigeration medium under the conditions of periodically generated disturbances*, Heat Transf. Eng., Vol. 32, 2011, pp. 359-368.

[40] Mikielewicz D., Klugmann M., Wajs J., *Flow boiling intensification in minichannels by means of mechanical flow turbulising inserts*, International Journal of Thermal Sciences, Vol. 65, 2013, pp. 79-91.

[41] Mikielewicz D., *Analytical model with nonadiabatic effects for pressure drop and heat transfer during boiling and condensation flows in conventional channels and minichannels*, Heat Transfer Engineering, Vol. 37, Issue 13-14, 2016, pp. 1158-1171.

[42] Kuczyński W., Charun H., *Experimental investigations into the impact of the void fraction on the condensation characteristics of R134a refrigerant in minichannels under conditions of periodic instability*, Arch. Thermodyn., Vol. 32, 2011, pp. 21-37, doi:10.2478/v10173.

[43] Bohdal T., Sikora M., Widomska K., Radchenko A.M., *Investigation of flow structures during HFE-7100 refrigerant condensation*, Arch. Thermodyn., Vol. 36, 2015, pp. 25-34, doi:10.1515/aoter-2015-0030.

[44] Kuczyski W., Charun H., Bohdal T., Kuczynski W., *Influence of hydrodynamic instability on the heat transfer coefficient during condensation of R134a and R404A refrigerants in pipe minichannels*, Int. J. Heat Mass Transf., Vol. 55, 2012, pp. 1083-1094, doi:10.1016/j.ijheatmasstransfer.2011.10.002.

[45] Dąbrowski P., Klugmann M., Mikielewicz D., *Selected studies of flow maldistribution in a minichannel plate heat exchanger*, Archives of Thermodynamics, Vol. 38, 2017, pp. 135-148.

[46] Kumar R., Singh G., Mikielewicz D., *A new approach for the mitigating of Flow Maldistribution in Parallel Microchannel Heat Sink*, Journal of Heat Transfer, Vol. 140, 2018, pp. 72401-72410.

[47] Kumar R., Singh G., Mikielewicz D., *Numerical study on mitigation of flow maldistribution in parallel microchannel heat sink: channels variable width versus variable height approach*, Journal of Electronic Packaging, Vol. 141, 2019, pp. 21009-21011.

[48] Dąbrowski P., Klugmann M., Mikielewicz D., *Channel blockage and flow maldistribution during unsteady flow in a model microchannel plate heat exchanger*, Journal of Applied Fluid Mechanics, Vol. 12, 2019, pp. 1023-1035.

[49] Radchenko A., Trushliakov E., Kosowski K., Mikielewicz D., Radchenko M., *Innovative turbine intake air cooling systems and their rational designing,* Energies, Vol. 13, Issue 23, 2020, No. 6201, doi:10.3390/en13236201.

[50] Radchenko R., Radchenko N., Tsoy A., Forduy S., Zybarev A., Kalinichenko I., *Utilizing the heat of gas module by an absorption lithium-bromide chiller with an ejector booster stage*, AIP Conference Proceedings, Vol. 2285, 2020, No. 030084, https://doi.org/10.1063/5.0026788.

[51] Radchenko N., Trushliakov E., Radchenko A., Tsoy A., Shchesiuk O., *Methods to determine a design cooling capacity of ambient air conditioning systems in climatic conditions of Ukraine and Kazakhstan*, AIP Conference Proceedings, Vol. 2285, 2020, No. 030074, https://doi.org/10.1063/5.0026790.

[52] Zhu Y., Jin X., Du Z., Fang X., Fan B*., Control and energy simulation of variable refrigerant flow air conditioning system combined with outdoor air processing unit*, Appl. Therm. Eng., Vol. 64, 2014, pp. 385-395.

[53] Zhou Y.P., Wu J.Y., Wang R.Z., Shiochi S., *Energy simulation in the variable refrigerant flow air-conditioning system under cooling conditions*, Energy Build., Vol. 39, 2007, pp. 212-220.